

**A 1000-YEAR OXYGEN ISOTOPE RECORD OF SOUTH AMERICAN  
HYDROCLIMATE FROM LAKE JUNIN IN THE CENTRAL ANDES OF PERU**

by

Kaitlin Clark

B.S., Union College, 2011

Submitted to the Graduate Faculty of the  
Kenneth P. Dietrich School of Arts and Sciences in partial fulfillment  
of the requirements for the degree of  
Masters of Science

University of Pittsburgh

2012

UNIVERSITY OF PITTSBURGH

Geology and Planetary Science

This thesis was presented

by

Kaitlin Clark

It was defended on

November 12, 2012

and approved by

Emily Elliot, Assistant Professor, Department of University of Pittsburgh, Department of

Geology and Planetary Science

Brian Stewart, Associate Professor, Department of University of Pittsburgh, Department of

Geology and Planetary Science

Mark Abbott, Associate Professor, Department of University of Pittsburgh, Department of

Geology and Planetary Science

Copyright © by Kaitlin Clark

2012

# **A 1000-YEAR OXYGEN ISOTOPE RECORD OF SOUTH AMERICAN HYDROCLIMATE FROM LAKE JUNIN IN THE CENTRAL ANDES OF PERU**

Kaitlin Clark, M.S.

University of Pittsburgh, 2012

The South American Summer Monsoon (SASM) provides the Peruvian Andes with precipitation during the austral summer. Over multidecadal timescales the SASM is influenced by sea surface temperature (SST) anomalies, land-sea temperature gradients, the El Niño Southern Oscillation (ENSO) and the location of the Intertropical Convergence Zone (ITCZ). Decadal to multi-decadal changes in SASM precipitation are documented by  $\delta^{18}\text{O}$  values of authigenic calcite precipitated from the waters of Lake Junin (11.0°S, 76.2°W), which is today a hydrologically open-basin lake system. This sediment record archives calcite-rich sediments that were used to determine the timing and magnitude of regional precipitation changes associated with variability of the SASM. Low  $\delta^{18}\text{O}$  values provide evidence for a strengthened monsoon system spanning the Little Ice Age (LIA) from AD 1250 to 1600. Following the LIA, higher  $\delta^{18}\text{O}$  values during the Current Warm Period (CWP) from AD 1850 to present are consistent with a time of decreased monsoon intensity. These data suggest that the SASM is sensitive to changes in the location of the ITCZ, which is influenced by Atlantic tropical SST anomalies controlled by Northern Hemisphere temperatures.

The Junin sediment record deviates from other regional paleoclimate records in AD 1932, recording a sharp and sustained decrease of  $\delta^{18}\text{O}$  values. This event is attributed to the construction of the Upamayo Dam, which resulted in the impoundment of waters from the Rio San Juan in Lake Junin, delivering river waters with low  $\delta^{18}\text{O}$  meteoric rainwater to the lake.

Trace metal data reveals a uniform and sustained enrichment of metal values beginning at 12 cm sediment depth (AD 1932), providing a reliable age-depth correlation between 12cm depth and the construction of the dam in 1932.

This project demonstrates that SASM variability is sensitive to ITCZ location, which is dominantly controlled by Atlantic SST anomalies. This relationship suggests that a continued warming of the north Atlantic will prove to be detrimental to tropical latitudes by reducing precipitation across the region.

## TABLE OF CONTENTS

<b>PREFACE.....</b>	<b>XI</b>
<b>1.0 INTRODUCTION.....</b>	<b>1</b>
<b>1.1 CLIMATE .....</b>	<b>2</b>
<b>1.2 SETTING.....</b>	<b>5</b>
<b>1.3 REGIONAL MINING HISTORY .....</b>	<b>8</b>
<b>1.4 REGIONAL PALEOCLIMATE ARCHIVES AND PAST RESULTS .....</b>	<b>10</b>
<b>2.0 METHODS .....</b>	<b>16</b>
<b>3.0 RESULTS.....</b>	<b>20</b>
<b>4.0 DISCUSSION .....</b>	<b>30</b>
<b>4.1 AGE MODEL.....</b>	<b>30</b>
<b>4.2 JUNIN-PUMACOCHA ISOTOPE COMPARISON .....</b>	<b>34</b>
<b>4.3 ENVIRONMENTAL ISOTOPES.....</b>	<b>36</b>
<b>4.3.1 Junin Core B <math>\delta^{18}\text{O}</math> record .....</b>	<b>36</b>
<b>4.3.2 Regional comparison of archive <math>\delta^{18}\text{O}</math> records.....</b>	<b>39</b>
<b>4.3.3 Sea surface temperature reconstructions and <math>\delta^{18}\text{O}</math> records .....</b>	<b>40</b>
<b>4.3.4 Carbon isotope variability in Junin Core B .....</b>	<b>41</b>
<b>5.0 CONCLUSIONS AND FUTURE IMPLICATIONS .....</b>	<b>44</b>

**BIBLIOGRAPHY..... 47**

## LIST OF TABLES

Table 1. Lake Junin sediment core data .....	6
Table 2. Radiocarbon ages and associated data from Lake Junin.....	20

## LIST OF FIGURES

Figure 1. Long-term mean precipitation map of South America during the austral summer and winter. The precipitation patterns track the movement of the ITCZ. Image from Vuille et al. 2005.....	4
Figure 2. Location map of Lake Junin and it's drainage basin. Image from Rodbell et al. 2011.....	7
Figure 3. Bathymetry map of Lake Junin with seismic data collected from 2008 and 2011. The sold black line is 4-24 kHz source; open circle black lines are from air gun seismic work. Image from Rodbell et al. 2011.....	8
Figure 4. Surface water samples from Lake Junin taken in July 2000 (triangles) and February 2001 (diamonds), and plot along the Local Evaporation Line (LEL). Surface water samples from the nearby Lake Pumacocha and the monthly precipitation averages from the Cerro de Pasco weathering station plot along the Local Meteoric Water Line (LMWL).....	13
Figure 5. Core location sites at Lake Junin.....	17
Figure 6. Age-depth model for Junin short core B generated by AMS radiocarbon dates.....	21
Figure 7. Age-depth model for Junin short core F generated by AMS radiocarbon dates.....	22

Figure 8. XRD intensity graphs for Lake Junin core B. Calcite peaks are labeled with a ‘C’. Intensity is unitless.....	24
Figure 9. Euhedral calcite from Junin short core B 33-34 cm.....	25
Figure 10. Downcore variations in %calcite, %TIC, %TOC, $\delta^{13}\text{C}$ , $\delta^{18}\text{O}$ for Junin short cores B, E, and F.....	28
Figure 11. The trace metal concentrations (ppm) of Co, Cu, Zn, Pb, Fe and Mn measured in core B. Trace metal data from Delman 2011.....	29
Figure 12. Comparison of the Junin core B $\delta^{18}\text{O}$ record with the Pumacocha $\delta^{18}\text{O}$ record.....	32
Figure 13. Pumacocha $\delta^{18}\text{O}$ record in blue. A 5-point moving average of the Pumacocha $\delta^{18}\text{O}$ record is overlain on the high resolution Pumacocha data.....	33
Figure 14. Comparison of isotope records from the central Peruvian Andes. (A) Huascaran (red) is an icecore record from Thompson et al. (1995); (B.) Pumacocha (blue) is a marl lake core record from Bird et al. (2011a); (C.) Junin (green) is a marl lake record from Seltzer et al. (2000).....	35
Figure 15. The Lake Junin core B $\delta^{18}\text{O}$ record compared to the $\delta^{18}\text{O}$ records from Pumacocha sediment core (Bird et al. 2011a), Cascayunga speleothem record (Reuter et al. 2009) and Quelccaya ice cap (Thompson et al. 2006). The four unit divisions are labeled. The data for Pumacocha, Cascayunga and Quelccaya has been smoothed using a 5-point moving average.....	38
Figure 16. Junin core B $^{13}\text{C}$ downcore variations. The $^{13}\text{C}$ values remain very positive between 12-128 cm. The excursion to lower $^{13}\text{C}$ values at 12cm is attributed to the construction of the Upamayo dam.....	43

## PREFACE

The completion of this thesis has been a collective effort. I would like to thank Mark Abbott for guiding me through this research project, and pushing me to achieve success. My family and friends have been a huge support over the past year and a half, and their constant phone calls and visits have been a huge motivator for me. My boyfriend, Greg, has been a continual support from the beginning, and has always believed in me. I would like to thank Mark's other graduate students for their help, especially Matt Finkenbinder who offered countless hours of help and served as a sounding board for all of my ideas and questions. I would also like to thank the University of Arizona Environmental isotope lab and the University of California at Irvine for radiocarbon for running my samples.

## 1.0 INTRODUCTION

The focus of my research is to document the timing, magnitude and rate of oxygen and carbon stable isotope changes in lacustrine calcite in three cores from Lake Junin for the last 1,000 years and to use these changes as a proxy for changes in lake water hydrology to identify wet/dry cycles. This study will provide a climatic history at decadal to multi-decadal scale resolution. Downcore variations in oxygen isotope compositions reveal more negative values during wet periods and more positive values during periods of aridity. Regional archives, including other lacustrine sediment records, ice cores and speleothems, show a similar pattern, validating the findings from Lake Junin sediments regarding the timing and magnitude of the inferred climatic changes.

Lake Junin is a hydrologically open basin lake, although during periods of high aridity, the lake level becomes so low that the outflow of the lake is cut off, and the basin tends to exhibit characteristics of a closed basin system. Previous work on Lake Junin (Seltzer et al. 2000) has focused on understanding climatic changes on millennial time scales, recording long-term changes in insolation and precessional forcing. This research will focus on understanding the precipitation-evaporation record of the past 1,000 years, and help to solidify the relationship between the intensity of the South American Summer Monsoon (SASM), the location of the Intertropical Convergence Zone (ITCZ), and north Atlantic temperatures and northern hemisphere sea surface temperatures (SSTs). The SASM and ITCZ are primary controls of

precipitation over South America, and therefore it is implicit that we understand their natural variability as many people rely on this water source for crops, hydroelectric power, tourism and personal consumption.

## 1.1 CLIMATE

Monsoon systems are seasonal changes in atmospheric circulation and subsequent precipitation caused by differential heating of land and sea surfaces. The Asian and African monsoon systems are well-understood phenomena in the northern hemisphere, while the South American Summer Monsoon is the dominant system in the southern hemisphere. During the austral summer, the Southeast Pacific Anticyclone combines with cold SSTs causing dry conditions in the western South American tropical continent, while the east develops a thermal heat low, characterized by warm and humid conditions in the lower troposphere (Lenters and Cook, 1997). North of the Anticyclone, strong easterlies cause a moisture flux into the tropical Andes. The Altiplano separates these two distinct climate regions, which receive  $200\text{mm yr}^{-1}$  in the southwest and  $800+\text{mm yr}^{-1}$  in the northeast (Garreaud et al. 2003). During the austral winter, the monsoon weakens and disappears as the Intertropical Convergence Zone (ITCZ) migrates north over the western Pacific and Central America.

Our understanding of how the SASM has changed over time has improved greatly over the years (Bird et al. 2011a, Bird et al. 2011b, Vuille et al. 2012, Zhou and Lau 1998). The SASM is the largest monsoon system in the Southern Hemisphere and is a major influence on the Amazonian hydrologic and biogeochemical cycles (Zhang et al. 2008, Shanahan et al., 2009).

The SASM is seasonal, with an observed spatial temporal pattern following the areas of the warmest SSTs (Vuille et al. 2012). The Intertropical Convergence Zone is a driving influence of SASM fluctuations (Bird et al. 2011a). The ITCZ is a low-pressure zone where convection causes warm air to rise and precipitate. The ITCZ migrates north and south, seasonally tracking regions with the warmest sea surface temperatures (Chiang and Bitz 2005, Vuille et al. 2012) (Figure 1). The El Nino Southern Oscillation (ENSO) influences both the SASM and ITCZ. During El Nino events, the Central Andes tend to experience drier conditions, while coastal Peru and the mid-latitudes are anomalously humid. These conditions are reversed during La Nina events (Garreaud et al. 2009). The convective activity over the SASM region is primarily controlled by the moisture flux influenced by the location of the ITCZ. Therefore, the location and strength of the ocean's ITCZ is of great importance when understanding the SASM on land (Garcia and Kayano 2010).

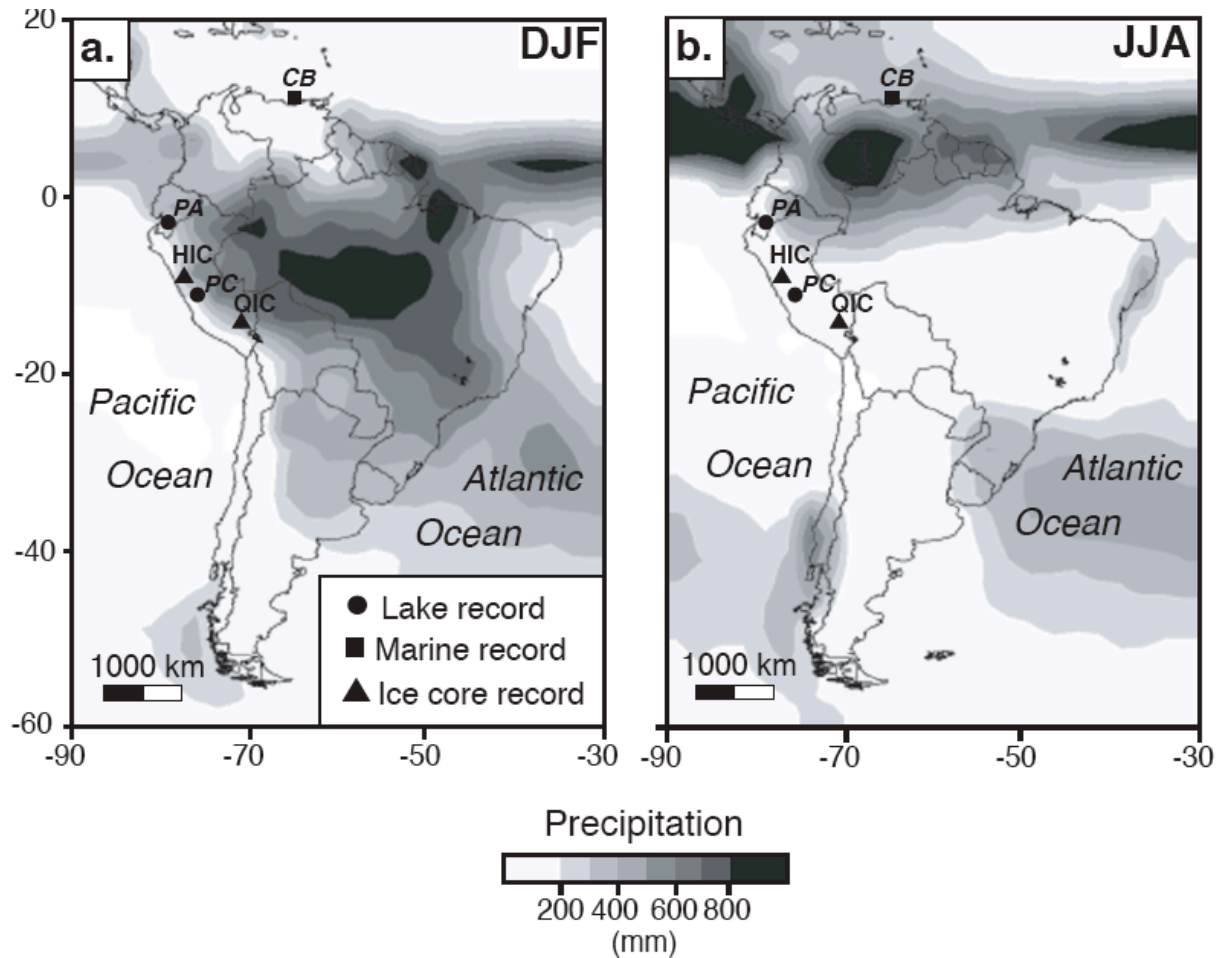


Figure 1: Long term precipitation over South American during the austral summer (DJF) and winter (JJA). The precipitation patterns track the movement of the Intertropical Convergence Zone (ITCZ). Figure from Vuille et al. 2003.

Many archives in the central Andes record periods of large-scale climatic changes driven by variations in the strength of the SASM in the Late Holocene, including: the Medieval Climate Anomaly (MCA) (900-1100 AD), the Little Ice Age (LIA) (1250-1600), and the Current Warm Period (CWP) (1850-today). These climatic events have been observed in multiproxy records from lacustrine sediment cores, ice cores and speleothems, all of which may record oxygen isotopic ratios with an annual- to decadal resolution. An investigation of these proxy records suggests that changes in the SASM intensity are regionally synchronous. SASM variability has

been attributed to a displacement of the ITCZ, caused by precessional forcing and changes in sea surface temperatures of the northern and tropical Atlantic Ocean (Abbott et al. 1997, Baker et al., 2001, Cruz et al. 2005). Understanding the temporal and spatial pattern of monsoonal variability can help determine the influence of sea surface temperatures, solar forcing and prevailing wind patterns on geographically different areas of the world.

## 1.2 SETTING

Lake Junín (11.00°S 76.19°W) is a large (300km<sup>3</sup>), open basin lake located in the southern Peru Altiplano at an altitude of 4,100 meters above sea level (Hansen et al. 1984) (7). The Altiplano is a large plateau located between the Cordillera Oriental and Cordillera Occidental (eastern and western mountain ranges, respectively) of the central Andes Mountains. The Junin Plain, formed during the late Pleistocene, was dammed by a combination of moraines and outwash fans at the time of glacial retreat, around 40,000 years BP (Hansen et al. 1984). Lake Junín has a surface area of approximately 300km<sup>3</sup> and a maximum water depth of 15m (Figure 3). The lake is underlain by siliciclastic carbonate and crystalline rocks in the eastern Cordillera, and Jurassic carbonates and Tertiary volcanics in the Western Cordillera. The lake has a small output flow in the northwest of the basin, draining to the Rio Montaro, a large Andean tributary that flows to the Amazon Basin (Wright 1983). Authigenic calcite precipitates in equilibrium with lake water in the summer during the height of biological productivity, which leads to small increases in pH. Although precipitation of calcite occurs annually, the amount per year is small, limiting our sampling resolution in Lake Junin to decadal to multidecadal resolution. Oxygen isotope ratios record moisture balance (P-E) conditions in the Lake Junin

region, a direct result of the intensity of the SASM and evaporative enrichment of  $\delta^{18}\text{O}$ . These measurements, coupled with radiocarbon dating methods, provide a continuous down-core record of climate variability of the Holocene for this location (Seltzer et al. 2000). Eight cores were taken from Lake Junin (Table 1), although only three short cores (B, E, F) were analyzed for interpretation because of their high carbonate concentration. Short core F is located 17.8 km from the inlet, the most central core location in the lake. Short cores B and E are located 25.51 km into the lake from the inlet, and approximately 6m apart from each other.

Table 1: Lake Junin sediment core data

Core	Core type	Length (cm)	Water depth (cm)	Year taken
A	Verschuren	42	238	2008
B	Verschuren	130	543	2008
C	Verschuren	58	488	2008
D	Verschuren	128	220	2008
E	Verschuren	108	544	2008
F	Verschuren	120	1083	2008
G	Verschuren	60	288	2008

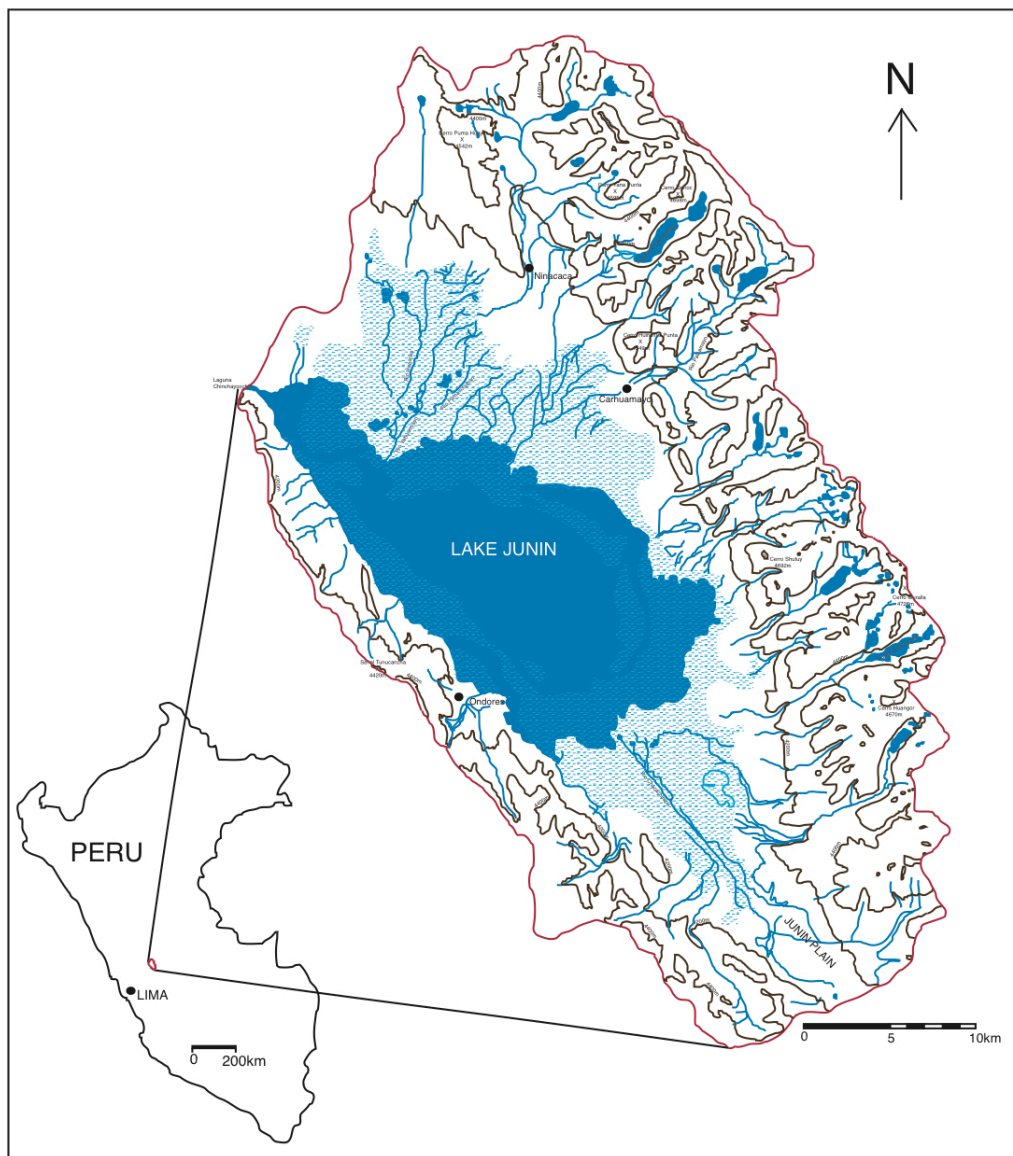


Figure 2: Location map of Lake Junin and its drainage basin. Figure from Rodbell et al. 2011.

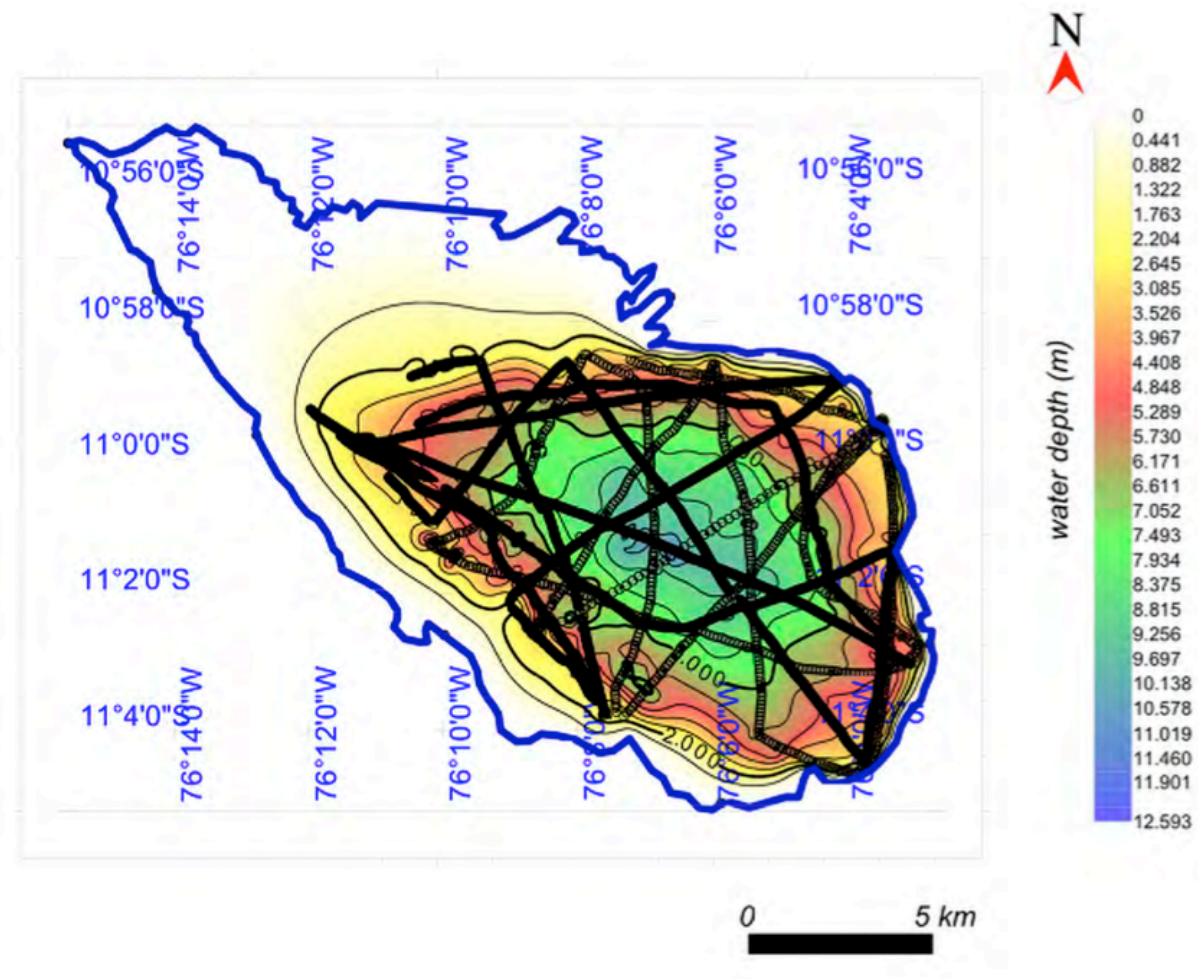


Figure 3: Bathymetry map of Lake Junin with seismic data collected from 2008 and 2011. The solid black line is 4-24 kHz source; open circle black lines are from air gun seismic work. Figure from Rodbell et al. 2011.

### 1.3 REGIONAL MINING HISTORY

Industrialization of the Central American Andes has resulted in the release of metals into the atmosphere, rivers and lakes from mining and smelting activities (Cooke 2008). The timing of this pollution can be used to help constrain the age of sedimentary layers, as the history of mining is reasonably well known from historical accounts. Located on the Altiplano in central Peru, Cerro de Pasco was first mined for silver by the Spanish in 1630AD, producing 11.2

million pesos in the last 5 years of the 1700s (Fisher 1977). Following the Peruvian War of Independence (1809-1824), mine owners rapidly acquired the land and began mining silver again. In the first two decades following Peruvian independence, Cerro de Pasco produced 65 percent of Peruvian silver, up from pre-war values of 40 percent. The volume of production at Cerro de Pasco grew extensively over the following centuries. Even after centuries of metal extraction and exploitation, Cerro de Pasco is still mined today, primarily for copper production (Benavides 1990).

The watershed of Lake Junin contains the Cerro de Pasco mine, and has suffered substantial anthropomorphic contamination due to the smelting, processing and subsequent deposition of metal tailings in the lake and surrounding tributaries. The construction of the Upamayo Dam in 1932 on the Rio Montaro has caused extreme contamination of Lake Junin (Delman 2012). The dam redirects the previously south-flowing Rio San Juan into Lake Junin, causing the northwest inlet of the lake to serve as both an inlet and outlet. This alteration of the hydrologic cycle ultimately caused the influx of waste-laden water from Cerro de Pasco to enter into the lake (O'Donnell 1997). Trace metal data from Core B lake sediments show a distinct and sustained increase in all metal concentrations at 12 cm depth. This increase is attributed to the construction of the Upamayo dam, and provides a well-constrained age-depth marker in the Junin Lake sediment, correlating 12 cm depth to 1932. Lake Junin is dammed during the austral wet season (October-April) to retain water for hydroelectric power during the dry season. This damming has caused the lake level to fluctuate 1.5 to 2m annually. The contamination of Lake Junin is visible in the red color of its surface waters and the decline of diversity of flora and fauna surrounding the basin.

## 1.4 REGIONAL PALEOCLIMATE ARCHIVES AND PAST RESULTS

Laminated lake sediments can provide annual to decadal resolution of oxygen isotope ratios from authigenic calcite ( $\text{CaCO}_3$ ) precipitated in the lake's water column if sedimentation rates are high enough and the water column is anoxic. Oxygen isotope values are important for understanding the prevailing precipitation and climatic patterns in a given area. There are two major factors that effect  $\delta^{18}\text{O}$  values of lake water: (1) the isotopic composition of input waters and (2) hydrologic processes, such as evaporation. Isotopic compositions of input waters are influenced by the  $\delta^{18}\text{O}$  values of precipitation, surface runoff and groundwater and these inputs can be altered by the origin of atmospheric moisture, air mass history and the seasonality of precipitation. This isotopic signature helps to decipher the geographic precipitation pattern over South America, as is controlled by the intensity of the SASM.

The main control of isotopic composition of water vapor transported over the Tropical Atlantic to the Peruvian Andes can be described as Rayleigh-type fractionation (Vuille and Werner 2005). Preferential removal of the heavy isotope of oxygen ( $^{18}\text{O}$ ) during precipitation enriches the remaining vapor in the lighter isotope ( $^{16}\text{O}$ ). This causes the  $\delta^{18}\text{O}$  precipitation values of an air mass to be more negative with more intense or prolonged rainfall. Monsoon intensity controls air mass trajectory and subsequent rainout, and therefore during periods of stronger SASM intensity, the  $\delta^{18}\text{O}$  values of precipitation falling over the central Andes becomes increasingly more negative. The isotopic composition of rainfall becomes more negative with increased precipitation; this process is called the 'amount effect' (Dansgaard 1964). Because of the amount effect, more positive values of  $\delta\text{D}$  and  $\delta^{18}\text{O}$  values are observed during months of less rainfall (austral winter), while more negative values of  $\delta\text{D}$  and  $\delta^{18}\text{O}$  are attributed to times of higher precipitation (Dansgaard 1964).

Determining if a lake basin is hydrologically open- or closed-basin is extremely important as it indicates whether or not the lake sediment stable isotopes are sensitive to evaporation (e.g. Bird et al. 2011a). Closed-basin lakes have no surficial outflow, and lake levels are controlled by the balance of precipitation and evaporation (P-E), thus evaporative enrichment of  $\delta^{18}\text{O}$  is the primary control of  $\delta^{18}\text{O}_{\text{calcite}}$  values. A closed basin lake precipitates authigenic calcite ( $\text{CaCO}_3$ ) in the spring and summer through photosynthetically induced biomediation (Kelts and Hsu 1978), and records evaporative or drought-like conditions. During drier climatic conditions,  $^{16}\text{O}$  is preferentially evaporated from the lake, leaving the lake water more enriched in  $^{18}\text{O}$  (Seltzer et al 2000).

Closed-basin lakes are characterized by more positive  $\delta^{18}\text{O}$  and  $\delta\text{D}$  lake water values, relative to the local meteoric water line (LMWL), which is shown Figure 4. The global meteoric water line (GMWL) represents the isotopic composition of global precipitation and represents an average composition of global terrestrial waters that have not been affected by evaporation. The local meteoric water line (LMWL) represents the local composition of terrestrial waters derived from data collected from local sites; the LMWL plots parallel to the GMWL and includes the effects of evaporation as the rainfall moves through the atmosphere. The local evaporation line (LEL) plots oblique (down and to the right) to the LMWL, showing that  $\delta\text{D}$  and  $\delta^{18}\text{O}$  values of closed basin lakes are predominantly controlled by evaporative enrichment, characterized by enrichment of both  $\delta^{18}\text{O}$  and  $\delta\text{D}$  in lake water.

Open-basin lakes have a surficial outflow and generally have a shorter water residence time, which limits the amount of evaporation that occurs, generally leading to more negative values of both  $\delta\text{D}$  and  $\delta^{18}\text{O}$ . Measured  $\delta\text{D}$  and  $\delta^{18}\text{O}$  values from open-basin lakes plot along the LMWL, parallel to the GMWL (Figure 4). This parallel, but offset dataset shows the isotopic

composition of the lake water tracking the seasonal variation in  $\delta^{18}\text{O}$  of precipitation, not evaporation (Bird et al. 2011b). Due to the similarity of the  $\delta^{18}\text{O}$  of the lake water and  $\delta^{18}\text{O}$  of precipitation, it can be assumed that any calcite precipitated from the lake is in isotopic equilibrium with the lake water and therefore is indicative of the isotopic composition of precipitation. Influenced by the amount effect, in an open-basin system,  $\delta^{18}\text{O}$  is more negative during the austral summer wet season, despite warmer temperatures, and more positive during the dry austral winter, when the temperature is cooler (Bird et al. 2011b).

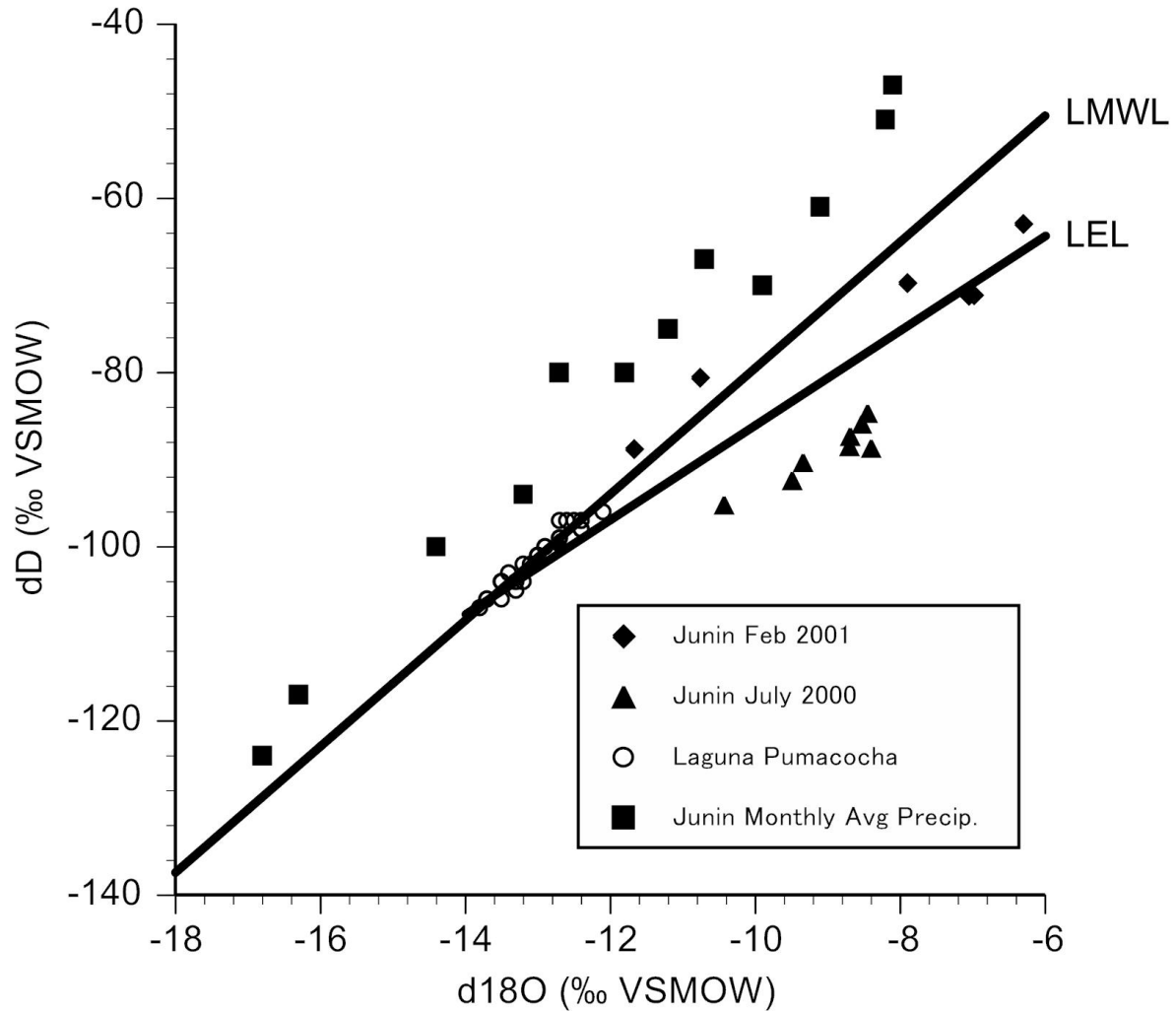


Figure 4: Surface water samples from Lake Junin taken in July 2000 (triangles) and February 2001 (diamonds), and plot along the Local Evaporation Line (LEL). Surface water samples from the nearby Lake Pumacocha and the monthly precipitation averages from the Cerro de Pasco weathering station plot along the Local Meteoric Water Line (LMWL).

Glaciers are another archive of oxygen and hydrogen isotopes although they are considerably higher in elevation than most lakes by 1000 to 1500 m. The  $\delta^{18}\text{O}$  record is fairly well established for the high latitude Greenland and Antarctic ice sheets (Alley 1997) which track atmospheric temperature. High altitude, low latitude regions are not as well understood. Thompson et al. (2006) suggest that  $\delta^{18}\text{O}$  of low latitude ice cores record changes in atmospheric

circulation on an annual to decadal time scale, and air temperature on longer time scales. Historically, the interpretation of oxygen isotopes from Andean glaciers is that more positive  $\delta^{18}\text{O}$  values signify warmer temperatures whereas a more negative  $\delta^{18}\text{O}$  values indicates cooler temperatures (Thompson et al. 2006). However, recent work suggests temperature changes may be minimal and most of the change in isotope values is related to moisture balance changes (Bird et al. 2011a; 2011b). Lower  $\delta^{18}\text{O}$  values observed in ice core records spanning in the LIA show a time of regional cooling and glacial advance, may also be related to wetter conditions. By using  $\delta^{18}\text{O}$  values, dust concentrations, aerosol chemistry and accumulation rates, a greater understanding of past climatic events can be more readily interpreted (Thompson et al. 1986, 2006). Although forcing mechanisms controlling  $\delta^{18}\text{O}$  values of tropical ice cores remains controversial, most agree that the large-scale dynamics of the tropical hydroclimate have shifted in the past 1,000 years (Thompson 2006).

Speleothems records from lowland caves are dated using U-Th dating methods and provide a more reliable age model compared to radiocarbon dating of lake sediments. Speleothems form by water percolation in limestone caves; therefore this isotopic record provides a signal of the intensity and frequency of precipitation events. Typically, a strong austral summer (October-April) precipitation is controlled by continental convection, and has a longer-term control that is influenced by ENSO. The precipitation pattern is extremely variable because of the topographic constraint and variable SST's of both the Atlantic and Pacific. Therefore, the recorded changes in precipitation are dependent on the temporal and spatial complexity of the region (Reuter et al. 2009). A speleothem from Cascayunga cave in northeast Peru records variability attributed to monsoon intensity over the past 2,000 years. Reuter et al. (2009) determined that on average, annual precipitation was 10 to 20% higher during the LIA

compared to the 20<sup>th</sup> century (CWP). This increase in annual rainfall is attributed to cooler north Atlantic SSTs. Oxygen isotope values from the LIA are an average 1.0‰ lower than the CWP (Reuter et al. 2009).

Lake Junin has been the focus of many studies, beginning with Hanson (1984), who showed that authigenic calcite is predominantly precipitated in the water column during non-glacial intervals. Seltzer et al. (2000) established an age-depth chronology for Lake Junin, based on radiocarbon analyses of organic matter and mollusc shells from a 19 m sediment core. The average rate of Holocene sedimentation was determined to be  $\sim 0.9$  mm/year <sup>14</sup>C years, with a minimal reservoir effect ( $< 60$  <sup>14</sup>C years). Carbonate analysis of the lacustrine sediment in the upper 11 m of the core revealed an overall trend from drier to wetter conditions from the late glacial through the Holocene, and suggest this change is due to the gradual increase in summer insolation since the early Holocene. An airgun seismic survey of Lake Junin revealed a sequence of 150 m of nearly undeformed sediment (Rodbell et al. 2011), suggesting that the sediment has recorded climatic variability over many hundreds of thousands of years.

In this study, coupled measurements of oxygen isotopic composition and accelerator mass spectrometry radiocarbon dated sediment provide a high-resolution record of climate variability in the past 1,000 years. Combining the Junin data with regional ice core and speleothem records thus provides a more comprehensive understanding of late Holocene climate change in this region.

## 2.0 METHODS

Eight short cores (A, B, C, D, E, F, G) were collected in the spring of 2008 by Donald Rodbell and Mark Besonen, from eight locations around Lake Junin using a Verschuren surface corer (Rodbell et al. 2011) (Figure 5). The cores were extruded in the field at 1-2cm sample intervals to ensure they would not be mixed during transport back to the University of Pittsburgh (Table 1).

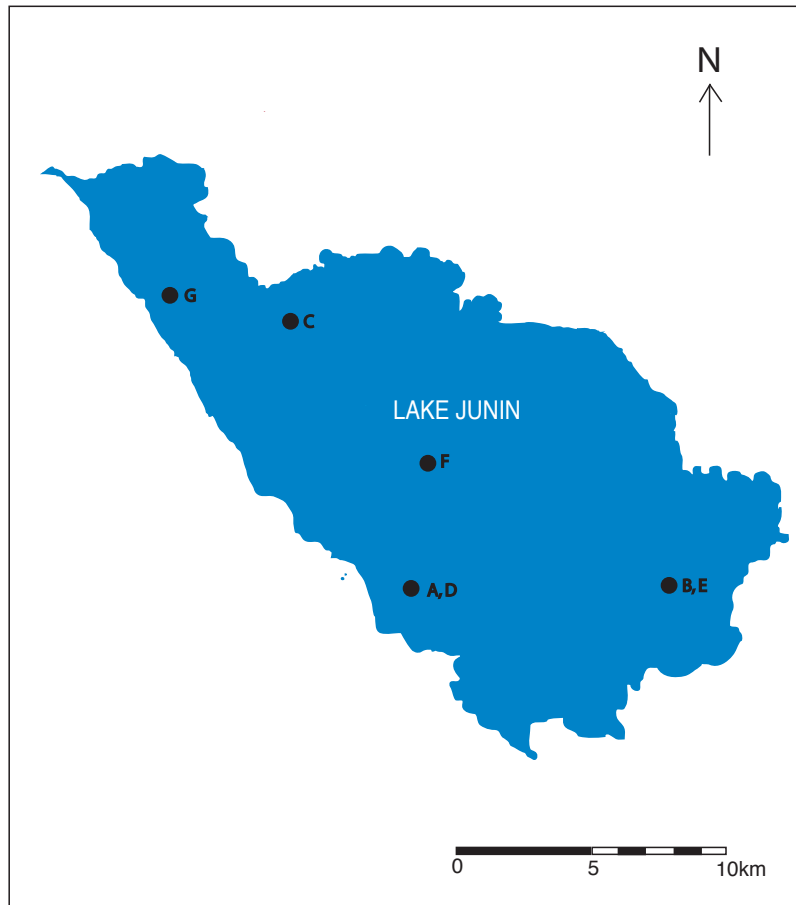


Figure 5: Core locations from 2008 from Lake Junin.

Multiple dating methods were used to correlate sediment core depths with ages. Lead-210 dating was attempted on Junin B-08 drives B and F. Twenty samples from both cores E and F were freeze-dried and equilibrated in a cold storage room at the University of Pittsburgh for three weeks. Lead-210 was then measured using a Canberra Germanium Detector at the University of Pittsburgh for 23 hours to detect gamma radiation. Following the constant rate of supply model adapted from Appelby and Oldfield (1983), sediment ages were determined.

Seven samples from Core B and four samples from Core F were prepped for AMS radiocarbon dating. Three of the samples from Core B are molluscs, and were pretreated at the University of Irvine, with a 10% HCl leach. The remaining seven samples were disaggregated in 7% H<sub>2</sub>O<sub>2</sub> overnight and wet-sieved to isolate discrete terrestrial macrofossils. Samples were then identified and handpicked under a stereomicroscope. These samples were then pretreated using the standard acid-base-acid procedure of Abbott and Stafford (1996) and sent to the Keck Center for Accelerator Mass Spectrometry at the University of Irvine for radiocarbon analysis.

Carbon and oxygen isotope samples were prepped at the University of Pittsburgh. The samples were covered in 7% H<sub>2</sub>O<sub>2</sub> for 24 hours to remove biologic carbonate. Samples were then sieved, and the <63 micron sample was bleached using a solution of 50% Clorox bleach and 50% deionized water for 6-8 hours. The samples were then centrifuged to decant the bleach and rinsed three times with deionized water. Finally, the samples were freeze-dried for 36 hours and homogenized.  $\delta^{18}\text{O}$  and  $\delta^{13}\text{C}$  of the carbonate samples were measured at the Environmental Isotope Laboratory at the University of Arizona using an automated carbonate preparation device (KIEL-III) coupled to a Finnigan MAT 252 gas-ratio mass spectrometer. The isotope ratio measurement is calibrated based on repeated measurements of NBS-18 and NBS-19.

X-ray diffraction analysis was first performed on three samples from Short Core B (33-34 cm, 62-64 cm, 126-128 cm) using a Philips X'pert X-Ray diffractometer for powder diffraction. The samples were pretreated using 7% H<sub>2</sub>O<sub>2</sub> to remove organic matter, and then rinsed with deionized water. Then the samples were frozen, freeze-dried and homogenized. This sediment was then packed into a metal stage slide for analysis. XRD results were analyzed to characterize the general mineralogical composition. The sample intervals from Short Core B were then

imaged using the Philips XL-30 field emission Scanning Electron Microscope (SEM) at the University of Pittsburgh's Department of Mechanical and Material Science.

Metal concentrations were measured by ICP-MS at Union college where concentrations of Co, Cu, Zn, Ba, Sr, Pb, Fe and Mn were measured. The flux of metal in six cores was determined, comparing Zn and Pb levels in Junin Core B to the Pumacocha lacustrine record. Flux was calculated by multiplying the bulk density of the sub sample by the sedimentation rate by the metal concentration at each sub-sample.

Carbon analysis was performed by UIC Coulometric Carbon Dioxide Coulometer at Union College by Erin Delman. Total carbon coulometry was used to acquire total inorganic carbon (TIC) and total organic carbon (TOC). These samples were then combined with 1.0 mL of high-purity HNO<sub>3</sub> and 9.5mL of deionized water and refrigerated for 24 hours. 1.0mL of the sample was then moved to the ICP-MS tube and diluted with 9.0mL of solution. The ICP-MS then analyzed the sediment for Co, Cu, Zn, Ba, Sr, Pb, Fe and Mn.

### 3.0 RESULTS

Lead-210 results were inconclusive, as the values of unsupported  $^{210}\text{Pb}$  were not detected above background levels. Radiocarbon dates (Table 2) were calibrated using CLAM mode, with IntCal09 and point-to-point linear interpolation (Blaauw 2010). Age-depth models from the AMS dates obtained for charcoal samples from Cores B and F are shown in figure 6 and 7, respectively.

Table 2: Radiocarbon ages and associated data from Lake Junin

Core	Sample depth (cm)	Material	$^{14}\text{C}$ age (BP)	$^{14}\text{C}$ age error	Median calibrated age (cal yrsBP)	2-sigma calibrated range (cal yrBP)
Core B	32-34	Charcoal	2010	50	1978	1873-2120
Core B	60-64	Charcoal	2435	20	2529	2365-2732
Core B	126-130	Charcoal	3785	25	4136	4055-4221
Core F	30-34	Charcoal	610	35		
Core F	53-57	Charcoal	1085	30	954	899-1010
Core F	91-94	Charcoal	3230	50	3454	3364-3567
Core F	116-119	Charcoal	3965	40	4391	4253-4492

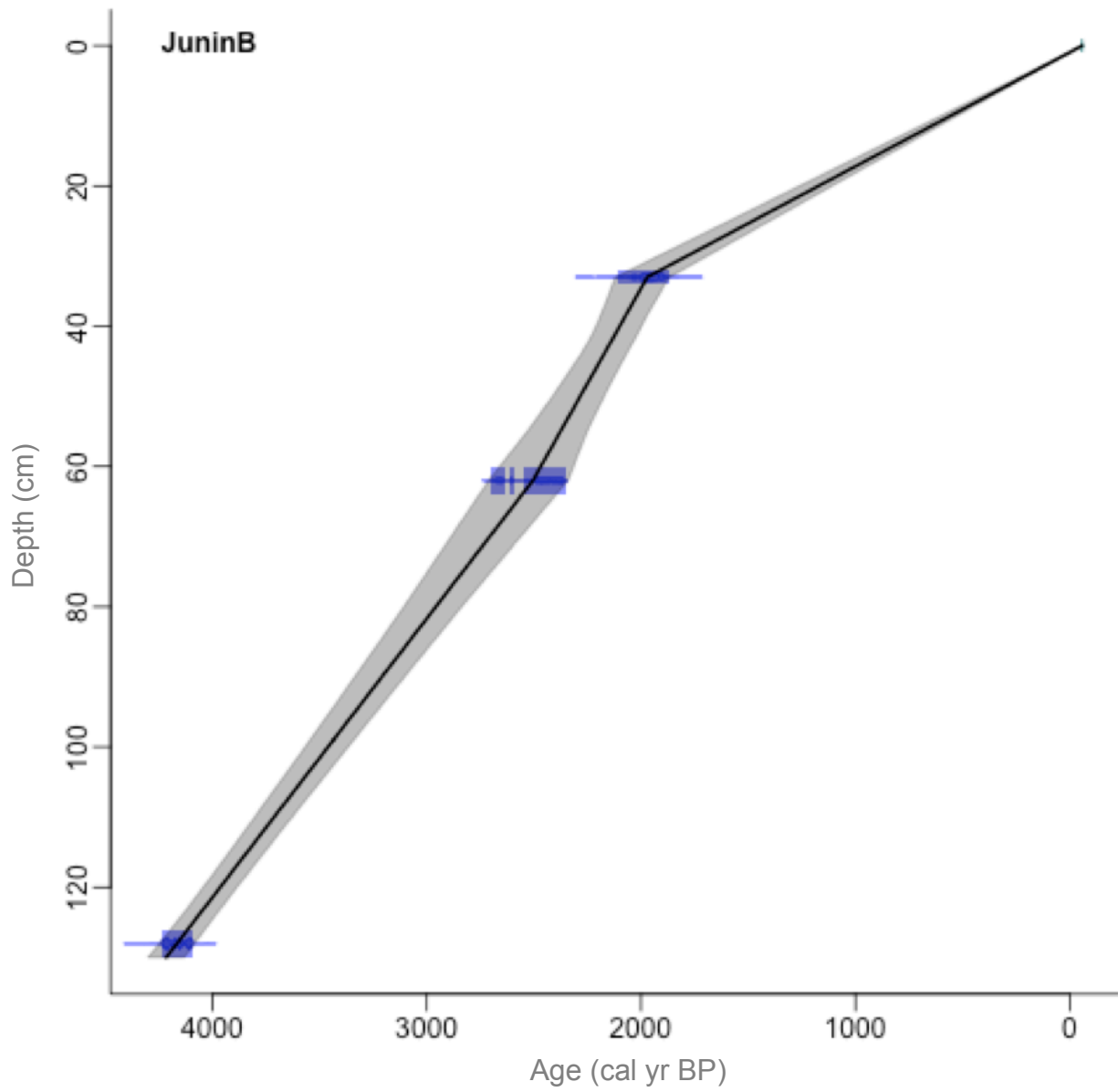


Figure 6: Age depth model for Junin short core B generated by AMS radiocarbon dates.

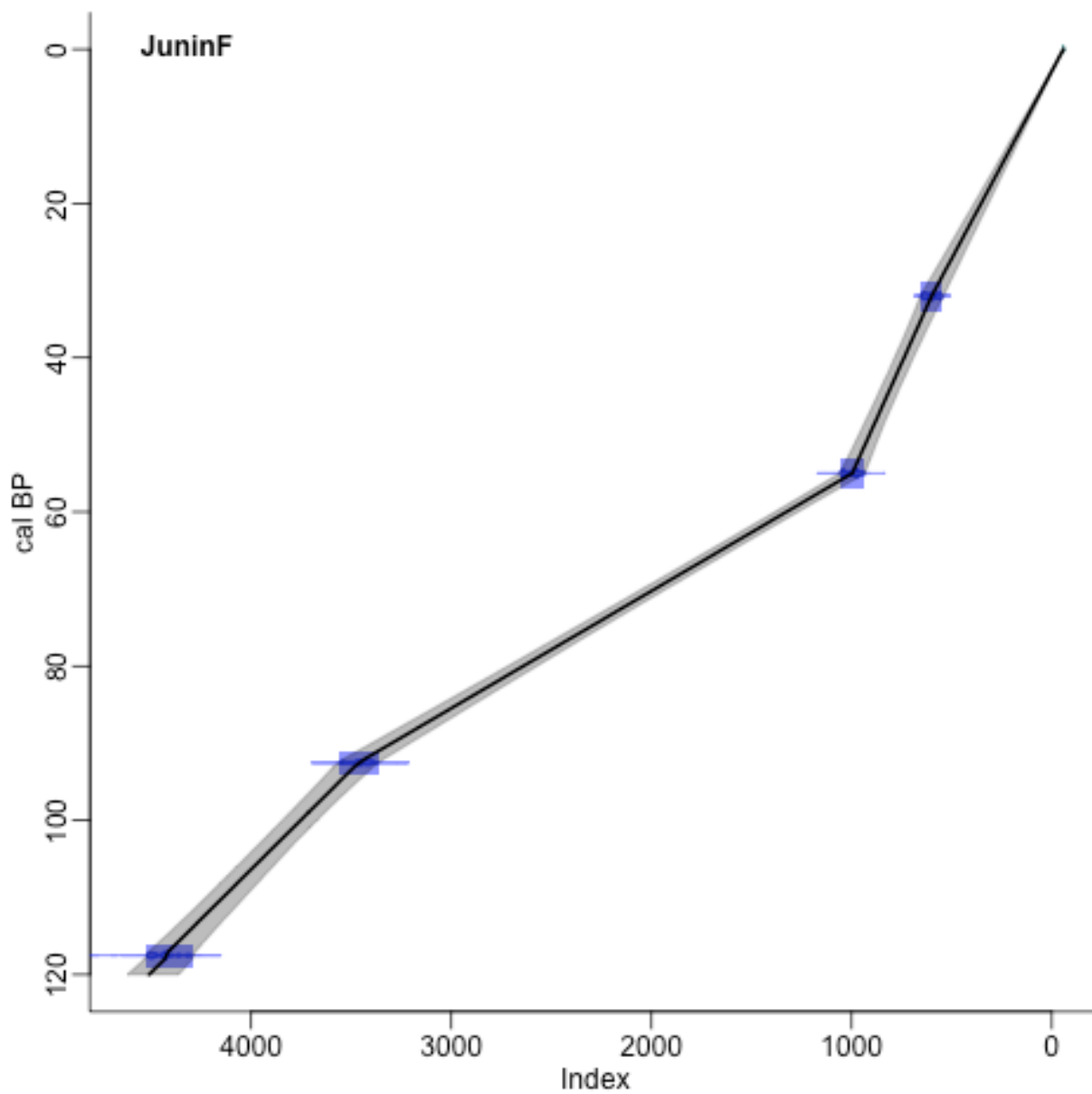


Figure 7: Age depth model for Junin short core F generated by AMS radiocarbon dates.

XRD analysis revealed that calcite is the dominant mineral in all three sample intervals from Junin Core B (Figure 8). These results coupled with SEM analysis, reveal that the precipitated carbonate crystals are predominantly euhedral calcite (Figure 9), and precipitated from the water column.

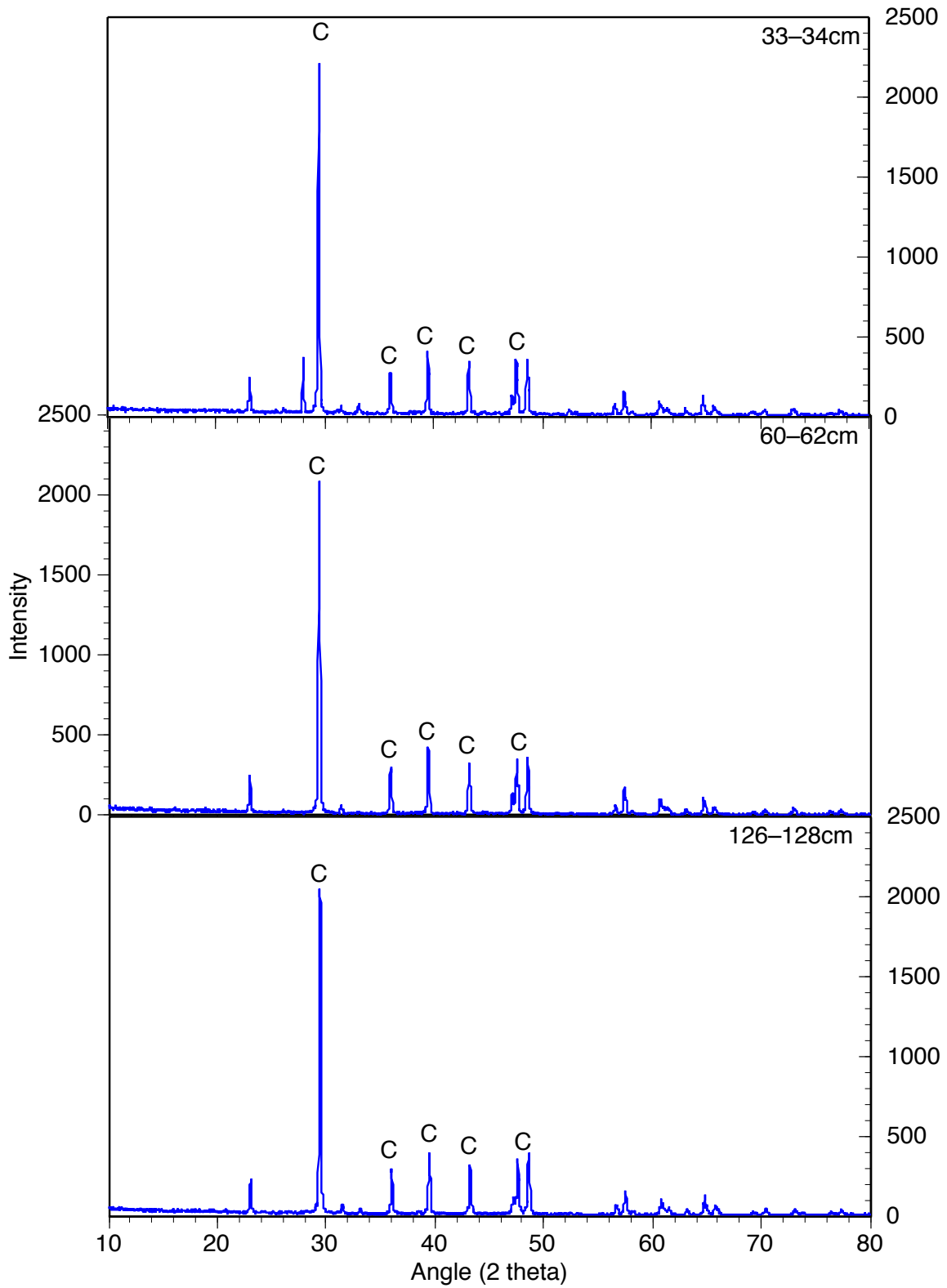


Figure 8: XRD intensity graphs for Lake Junin core B. Calcite peaks are labeled with 'C'. Intensity is unitless.

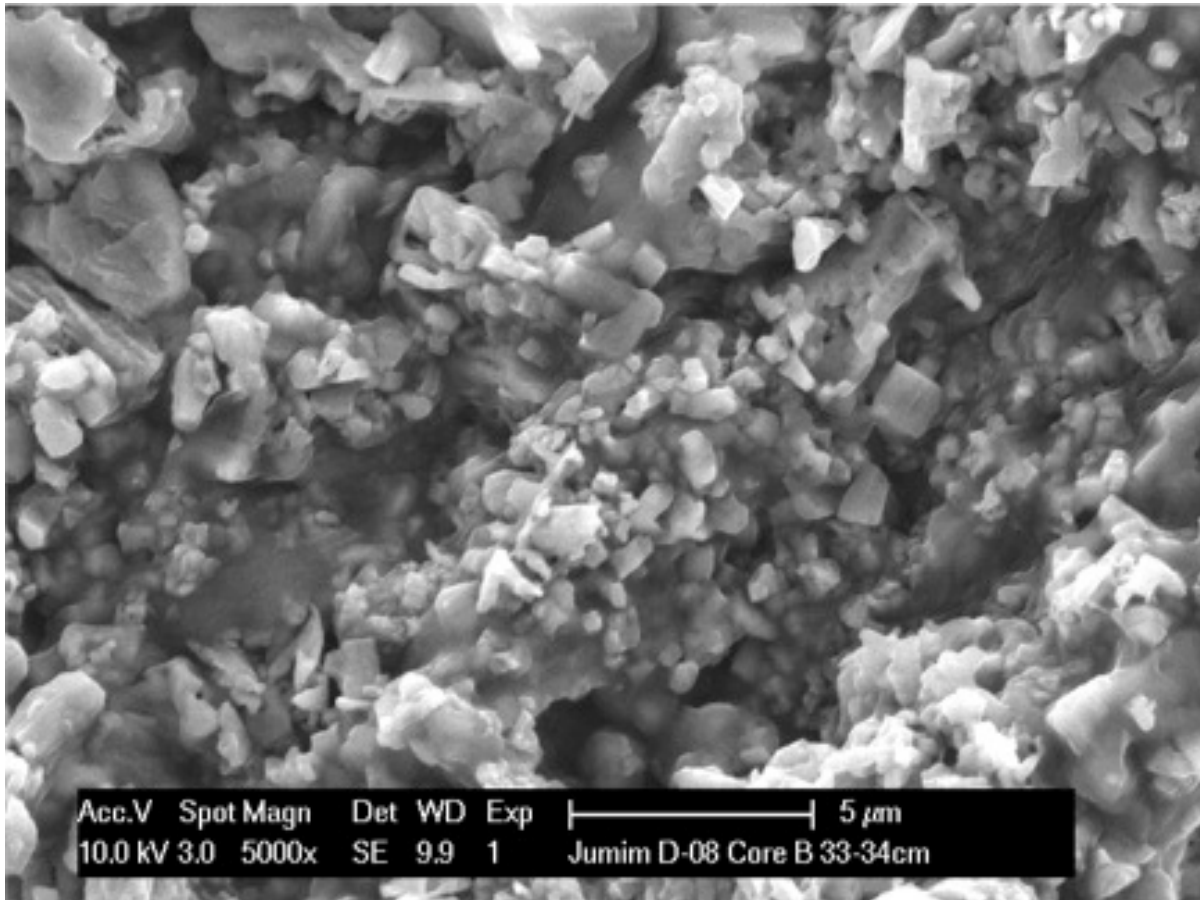


Figure 9: Euhedral calcite from Junin short core B 33-34cm.

Three cores, core B, core E and core F, were analyzed for % calcite, %TIC, %TOC,  $\delta^{13}\text{C}$  and  $\delta^{18}\text{O}$ . The measurements for each core exhibit similar trends. The %TIC is calculated by the following equation (Myrbo 2004):

$$\%TIC = \{(\mu\text{g C}) - \mu\text{g C}[\text{blank value}] / \mu\text{g} [\text{sample weight}]\} \times 100$$

This equation demonstrates that % calcite and %TIC downcore values will be offset but covary. Therefore, when presenting the data, I will only refer to the %calcite in each core. TIC is calculated by subtracting TOC from TC. Therefore, The TIC and TOC values mirror one

another. On average, %TOC increases up-core, while % calcite and %TIC decrease up-core (Figure 10).

Oxygen isotope values of Core B range from -7.9 to -5.3‰ over 130 cm depth. The record shows four distinct units and an overall arc-like trend to more positive values. Unit one starts at the bottom of the core, from 110-130 cm. This event has a maximum enrichment of -5.3‰, and values within this interval remain steady around this enrichment (more positive) value. The second unit starts at 110 cm with the most enriched  $\delta^{18}\text{O}$  value, -5.4‰, and is characterized by the most depleted values in the core. The third unit begins at 30 cm, with the most enriched  $\delta^{18}\text{O}$  value of -5.8‰ at 27 cm. The fourth and final event is the most pronounced change in the core. The  $\delta^{13}\text{C}$  values remain constant throughout the first three units. The final unit starts at 12 cm, as the  $\delta^{18}\text{O}$  values abruptly shift to extremely depleted values, reaching a value of -7.9‰ at the very top of the core. The  $\delta^{13}\text{C}$  values for unit four make a large shift at 12 cm, from 13.8‰ to 3.8‰ at the core top.

The top of core E was not properly extruded in the field and therefore the analysis begins at 20cm. From 55-108 cm the calcite ranges from 74.2%-83.0%,. From 20-55 cm there is a general trend of decreasing calcite, ranging from 79.3% to 67.0%. %TOC mirrors %calcite, with little variation, ranging between 7.3%-11.5% from 55-108 cm. From 55cm to the core top, there is an increasing trend ranging between 9.4% and 13.0%.  $\delta^{13}\text{C}$  has an arc like trend, with the greatest depletion in the middle of the core. Between 35 and 108 cm, there is a gradual trend to more depleted values ranging from 11.7‰ to 13.8‰. At 35 cm, the  $\delta^{18}\text{O}$  values begin trending to greater enrichment, reaching a maximum enrichment value of 14.3‰ at 21 cm. Finally,  $\delta^{18}\text{O}$  values exhibit a trend to more depleted values up core, with a range of values between -4.6‰ to -7.5‰

Core F has the most variable downcore record of the three cores. Calcite has an arc-like trend, with the lowest values (41.2%) at 112 cm and reaching 0% twice at 55 cm and 22 cm, which could be attributed to inaccuracies in the measurements. % Calcite spikes at 39cm, with a value of 72.7%, and continues to more positive values until the core top. %TOC mirrors calcite, exhibiting a general trend to more positive values toward the core top.  $\delta^{13}\text{C}$  values remain steady, with values between 9.2‰ and 11.8‰, with a sharp increase to 12.7‰ at 38.5 cm. Above this interval,  $\delta^{13}\text{C}$  values decline to the core top.  $\delta^{18}\text{O}$  values range between -7.2‰ and -5.3‰ from the base of the core, until 40.5 cm where values reach -4.6‰, the most enriched value in the core. Values deplete upcore, reaching the most depleted value of -9.4‰ at 14.5 cm

The trace metal data shows obvious trends in core B. Core B is located ~25 km from the lake inlet. Trace metals concentrations remain low (background) until 12 cm, when all metal concentrations increase sharply. At 9.5 cm, Mn spikes at  $4.55 \times 10^4$  ppm. At 3.5cm, Fe= $2.33 \times 10^4$  ppm, Co=23.5 ppm Cu=477 ppm, and Zn= $5.51 \times 10^4$  ppm. Finally, at 2.5cm, Pb concentrations reach 238 ppm (Figure 11).

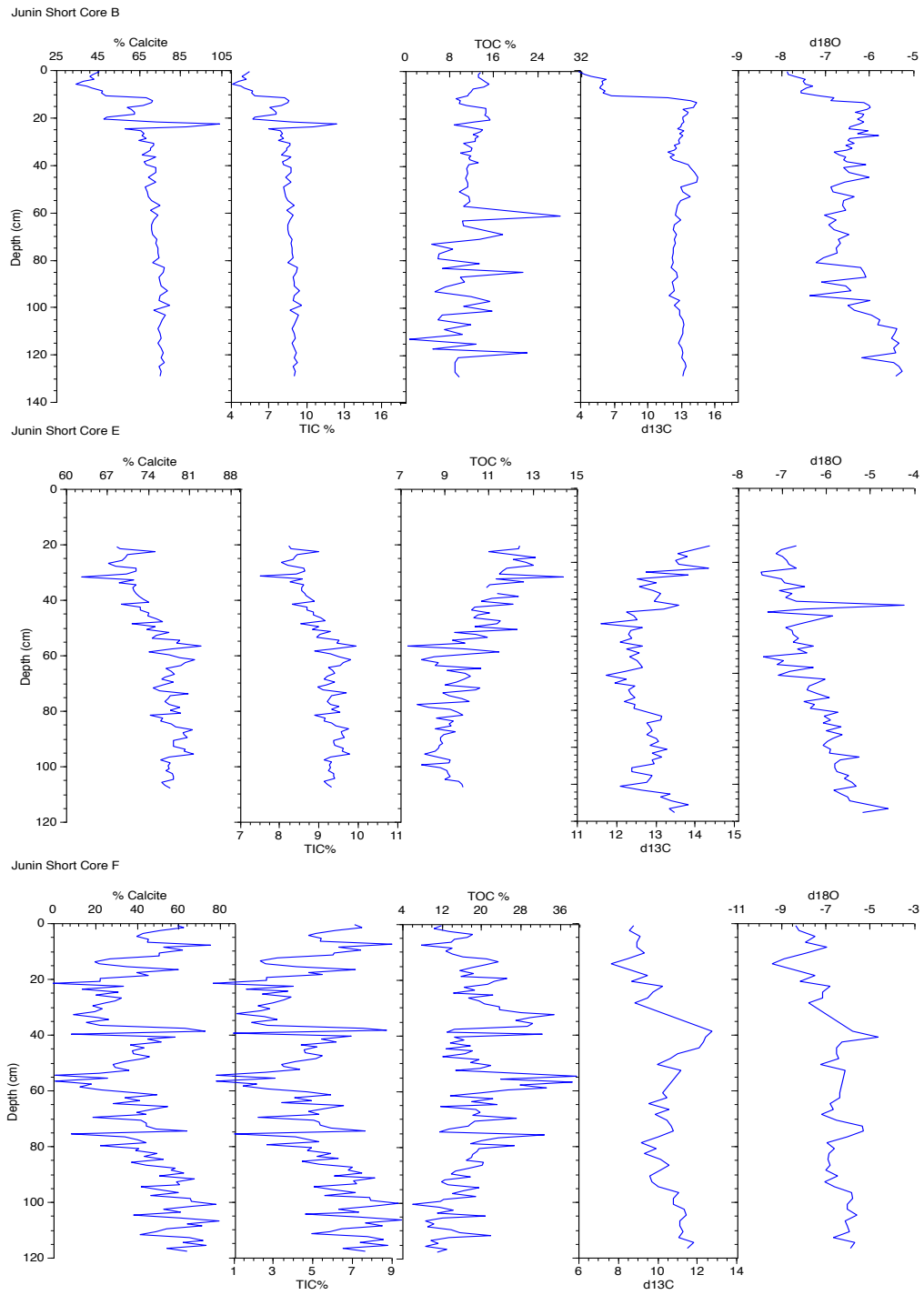


Figure 10: Downcore variations in % calcite, % TIC, % TOC,  $\delta^{13}\text{C}$ ,  $\delta^{18}\text{O}$  for Junin short cores B, E, and F.

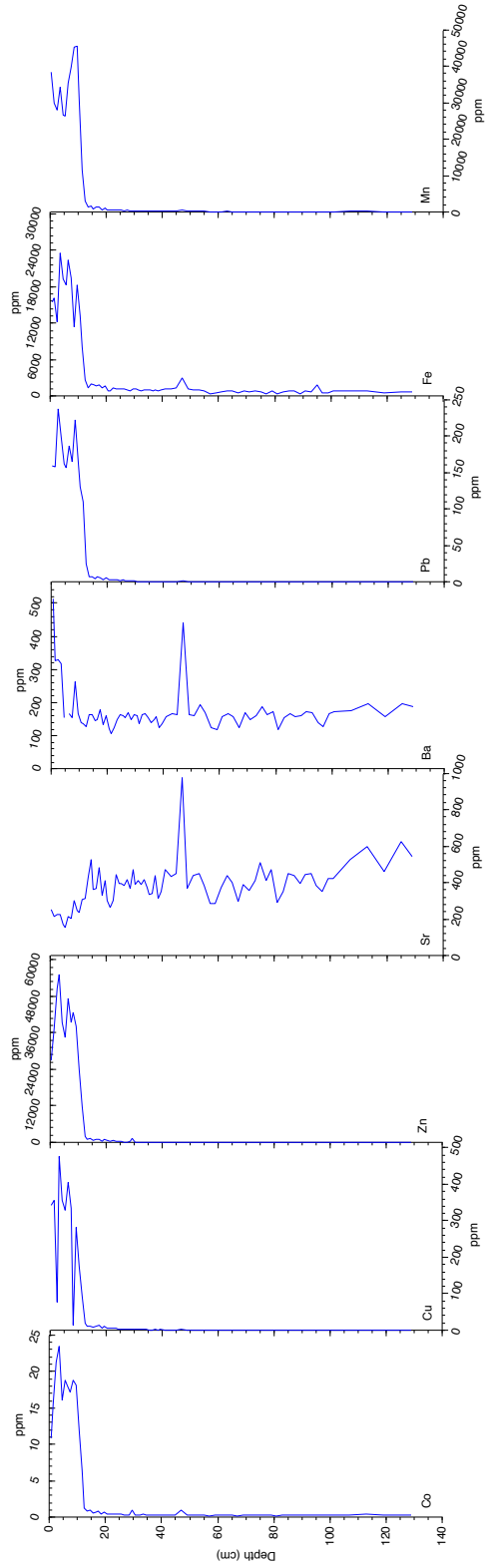


Figure 11: The concentrations (ppm) of Co, Cu, Zn, Pb, Fe and Mn in Core B (Delman 2011).

## **4.0 DISCUSSION**

### **4.1 AGE MODEL**

Junin Core B is located far from river inputs in the SE section of the Lake Junin basin. Consequently, the 128 cm long sedimentary section in Core B is continuous, well-preserved, and provides a high-resolution record for the past 1,000 years. In addition, Core B is the most distal (25 km) from the input stream and Upamayo dam, allowing for the record to be nearly undisturbed. Accordingly, focus will be placed on Core B for the development of the geochronology of this stratigraphic section.

The age model generated by AMS radiocarbon dates (Figure 6, 7, Table 2) from Core B is discordant with previously published results (Seltzer et al. 2000). The basal radiocarbon age for Core B is 4,160 cal BP (-2210 AD/BC). When compared to the results generated by Seltzer et al. (2000), who radiocarbon-dated molluscs and macrofossils at similar and deeper depth horizons from Lake Junin, the measured ages from this study appear significantly too old. Furthermore, Seltzer et al. (2000) validated their radiocarbon chronology by using uranium-thorium dating methods on calcite.

In order to explain these discrepancies, we must understand the problems associated with radiocarbon dating in a lacustrine environment. Radiocarbon dating requires the measurement of  $^{14}\text{C}$  preserved in organic materials, measuring the amount of radioactive decay in order to calculate the given age for the sample. Plants uptake atmospheric carbon through photosynthesis and animals ingest the plant material, thereby incorporating a known amount of radiocarbon from the plants. When the organism dies, this carbon exchange stops and  $^{14}\text{C}$  begins to decay radioactively. By measuring the parent-daughter ratio in a given sample you can then calculate the time of the organism's death. If an organism dies and is preserved on the landscape and is subsequently eroded and redeposited in lake sediment at a later time, the sediment will have an anomalously old radiocarbon date. There is evidence of large erosional events at Lake Junin, as seen by the down cutting of input stream channels and bi-annual large-scale lake level fluctuations (1-2m) controlled by the Upamayo dam (Rodbell et al., 2011). The marsh-like catchment surrounding the lake coupled with the annual change in lake level could also supply old carbon. If the down cutting of the surrounding wetlands by streams erodes old soils or marsh vegetation and redeposits this material in the lake, then it could account for erroneously old radiocarbon ages. The high altitude environment of the lake is also conducive to large-scale erosional events by wind and heavy rain.

Bird et al. (2011a, 2011b) developed a  $\delta^{18}\text{O}$  record with  $^{14}\text{C}$  and  $^{210}\text{Pb}$  age control for Lake Pumacocha located 20km NW of Lake Junin. Studies have indicated that Lake Pumacocha and Lake Junin are influenced by the same climatic forcing because of their close proximity and comparable environments (Delman 2011, Rodbell et al. 2011). Carbonate isotopes were analyzed for both lakes and the data exhibits similar, but offset trends in the  $\delta^{18}\text{O}$  record. Because of these similarities, an age-depth correlation between the two lakes was used to

identify similar trends of  $\delta^{18}\text{O}$  variability through time and identify common points that were used to tie the records together and produce an age model (Figure 12). The Pumacocha data has been resolved to a 5-point moving average for a better comparison to the Junin core B data (Figure 13)

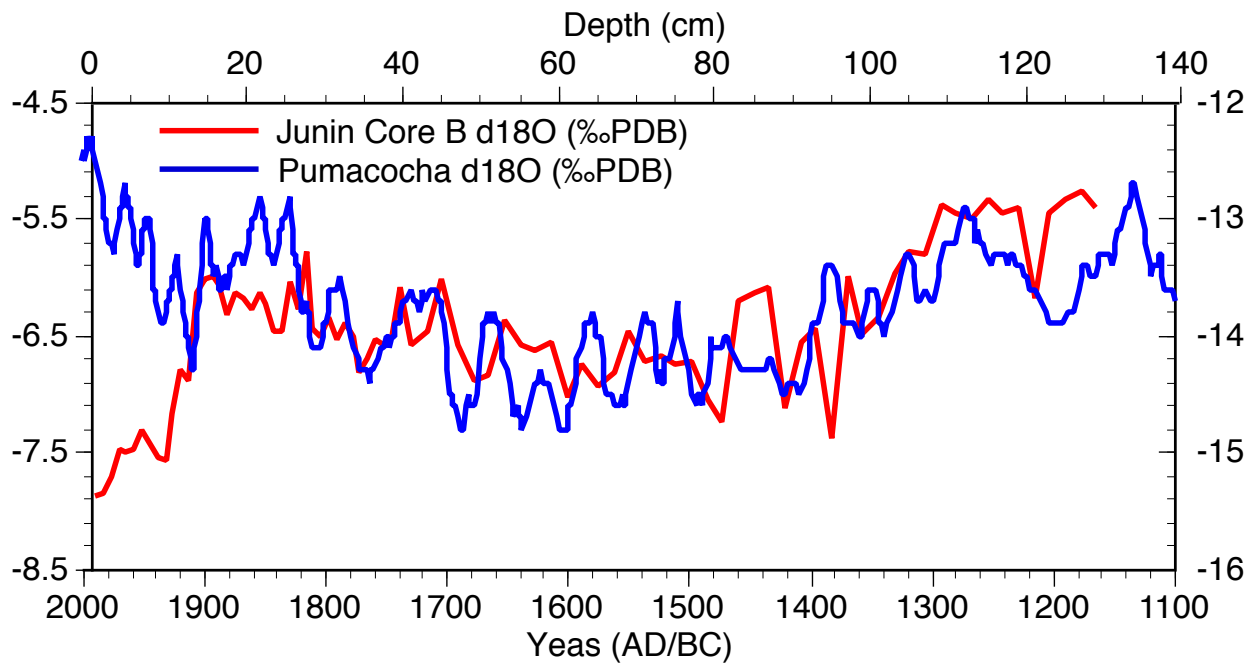


Figure 12: Comparison of the Junin core B  $\delta^{18}\text{O}$  record with the Pumacocha  $\delta^{18}\text{O}$  record.

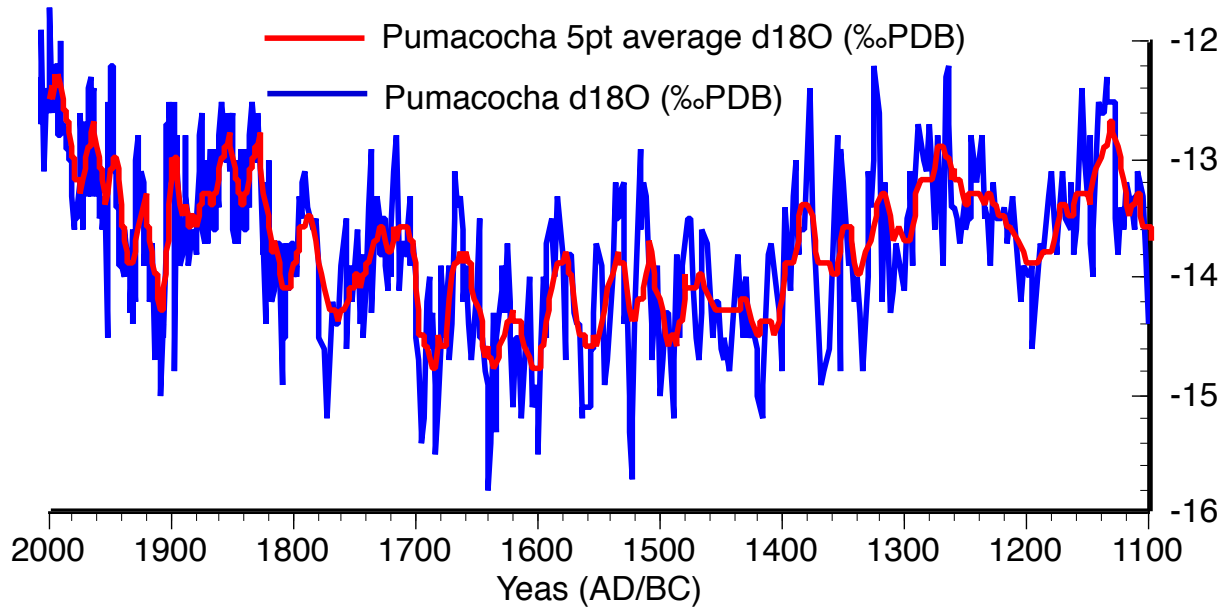


Figure 13: Pumacocha  $\delta^{18}\text{O}$  record in blue. A 5-point moving average of the Pumacocha  $\delta^{18}\text{O}$  record is overlain on the high resolution Pumacocha data. The 5-point moving average data will be used for comparison to the Junin  $\delta^{18}\text{O}$  record.

Supporting evidence for this approach comes from the trace metal data for Core B, which also suggests the radiocarbon age model is incorrect. Trace metal levels in Lake Junin have increased by up to three orders of magnitude, starting at 12cm depth in Core B (Delman 2011) (Figure 11). This level of metal contamination is unprecedented in the lake and can be attributed to the construction of the Upamayo dam on the Rio San Juan in 1932 AD. The molluscs dated at and around 12 cm depth (~1932) appear to be anomalously old (1216 AD, 1095 AD, 698 AD), and therefore I chose to do a point-to-point correlation between the Junin and Pumacocha oxygen isotope record. Both records show similar trends as well as a distinct deviation at 12cm depth, which is understood to be the time of dam construction. There are several possibilities of age

models for this sediment core and I have chosen to interpret the data based on one model in order to be consistent in interpreting the isotopic record.

Thus, coupling the metals data with the age-model of Lake Pumacocha provides the age-depth model used for Lake Junin Core B. The metal spike seen in Lake Junin sediments occurs at 12cm depth, corresponding to an age of ~1932 AD using the Pumacocha age-model. The Upamayo Dam was constructed in 1932 AD, causing metal tailings to be deposited in the lake, thus providing strong evidence for correlation.

## 4.2 JUNIN-PUMACOCHA ISOTOPE COMPARISON

The  $\delta^{18}\text{O}$  record of regional lake, ice and speleothem archives reveals a relatively synchronous transition from drier to wetter conditions from the early to late Holocene, respectively (Figure 14). The hydrologic mass balance of open- and closed-basin lakes is well understood and is important when interpreting  $\delta^{18}\text{O}$  values of lake water. Open-basin lake systems track changes in meteoric precipitation composition, while closed basin systems are controlled by evaporative enrichment (aridity); therefore, drier conditions in the early Holocene would cause a significant divergence in  $\delta^{18}\text{O}$  values between open- and closed-basin systems. A transition to wetter conditions in the late Holocene would result in a subdued evaporative effect in a closed basin system, causing the  $\delta^{18}\text{O}$  values in Lake Junin and Lake Pumacocha to record similar, but offset, isotopic compositions. As mentioned previously, during wetter times, the outflow channel to Junin remains active due to the high lake level, while during drier, more arid times, this channel becomes inactive due to a lower lake level. The isotope record for Lake

Junin Core B extends only to 1,000 AD, a period which is characterized by more precipitation (relative to the early Holocene), and therefore the Junin record can be interpreted as a balance of precipitation-evaporation, with an overprint record of SASM intensity.

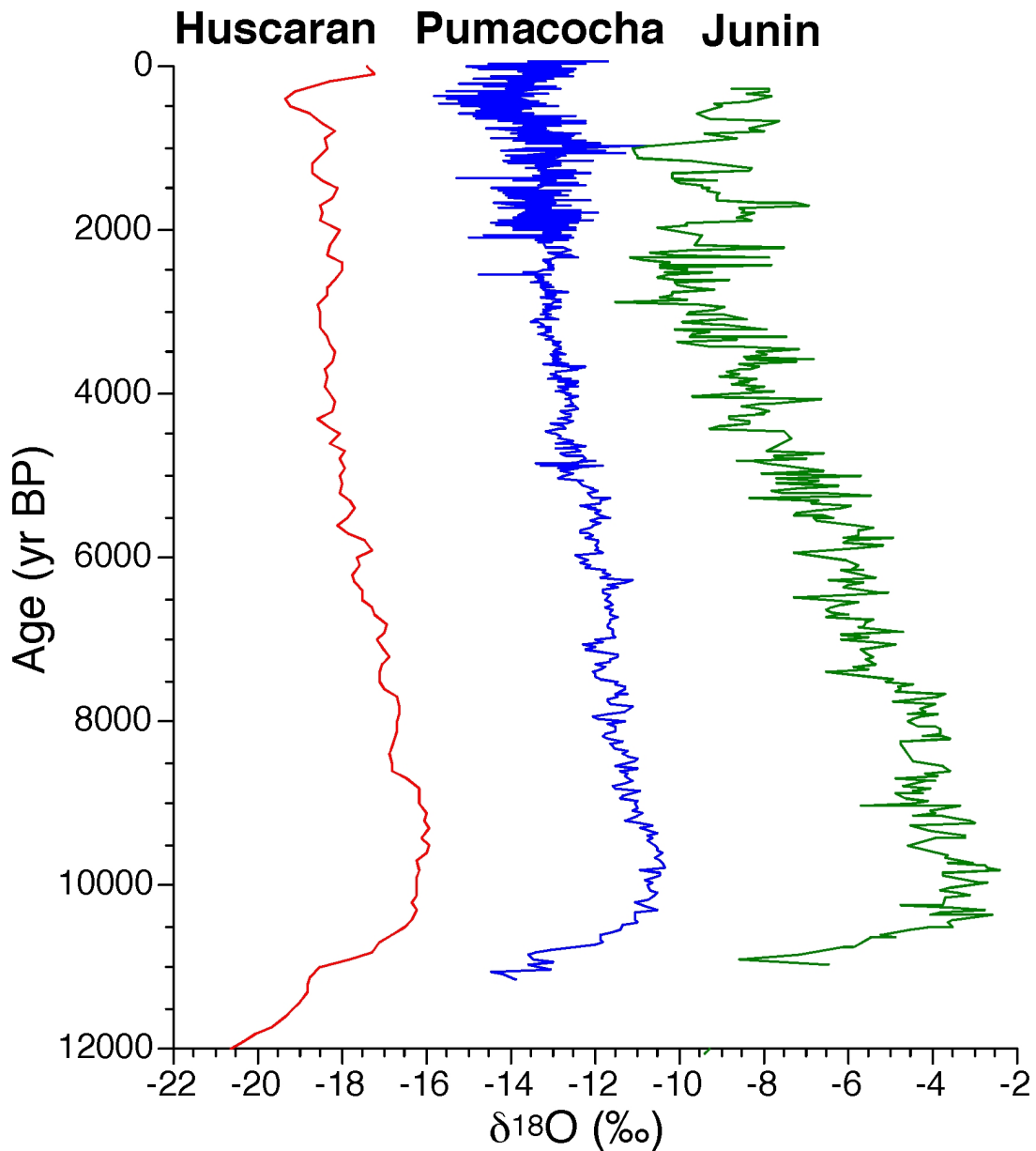


Figure 14: Comparison of isotope records from the central Peruvian Andes. (A) Huascarán (red) is an icecore record from Thompson et al. (1995); (B.) Pumacocha (blue) is a marl lake core record from Bird et al. (2011a); (C.) Junin (green) is a marl lake record from Seltzer et al. (2000).

## 4.3 ENVIRONMENTAL ISOTOPES

### 4.3.1 Junin Core B $\delta^{18}\text{O}$ record

The Junin isotope record is validated by the Pumacocha  $\delta^{18}\text{O}$  record (Bird et al. 2011) and shows similar trends with the Cascayunga cave and Quelccaya ice core  $\delta^{18}\text{O}$  records (Figure 15). While these regional archives record Holocene scale climatic changes, the Junin short Core B is limited to the past 1,000 years. Variations in  $\delta^{18}\text{O}$  values of Lake Junin Core B are interpreted to represent monsoon intensity. High (more positive)  $\delta^{18}\text{O}$  values represent a period of reduced monsoon intensity, while lower (more negative)  $\delta^{18}\text{O}$  values represent an increase in SASM intensity.

Unit I (1100-1250 AD) corresponds to the tail end of the Medieval Climate Anomaly (MCA) a period of high aridity and evaporation coupled with decreased monsoon intensity and precipitation. Higher, more positive  $\delta^{18}\text{O}$  values during this time are interpreted as a warm, dry period in the regional archives (Figure 15).

Unit II (1250-1600 AD) is characterized by maximum the lowest  $\delta^{18}\text{O}$  values, associated with the Little Ice Age (LIA) and a time of increased SASM intensity. Sea surface temperature (SST) reconstructions show that the north Atlantic cooled while the tropics experienced El Niño like conditions (Sachs et al. 2009). Archive records from the tropics suggest a southward displacement of the Intertropical Convergence Zone (ITCZ) during this time, which is consistent

with northern hemisphere (NH) cooling. Lake Junin  $\delta^{18}\text{O}$  values record this event, agreeing with the interpretation of a wetter LIA period, associated with a stronger SASM.

Unit III (1600-1932 AD) is recognized as the Current Warm Period (CWP). Sustained enrichment in  $\delta^{18}\text{O}$  values, as seen in the Lake Junin record, is indicative of a long-term weakening of the SASM. Due to the warming of the north Atlantic and the NH, a northward shift of the ITCZ would subsequently cause a weakened state of the SASM. The exact timing of this event is variable among climatic archives, but its sustained presence is supported by many studies (Figure 15) (Bird et al. 2011a, Bird et al., 2011b, Reuter et al. 2009, Vuille et al. 2012).

Unit IV (after the 1932 AD dam construction) shows a sharp transition to more negative  $\delta^{18}\text{O}$  values in the core. This deviates from the proxy data from the other regional archive records (Figure 15) and is the most distinct and sustained transition in core B. This transition is attributed to anthropogenic pollution caused by the construction of the Upamayo dam and subsequent deposition of mining tailings and waste being redirected and deposited into the lake. The construction of the Upamayo dam in 1932 is seen by a transition to low  $\delta^{18}\text{O}$  values and is also supported by the peak in trace metal data. The damming of the lake has caused the Rio San Juan to be redirected to flow into Lake Junin and subsequently adds a large flux of extremely negative  $\delta^{18}\text{O}$  meteoric water into the lake. This period of anthropogenic pollution is an isolated event attributed to local mining pollution and dam construction.

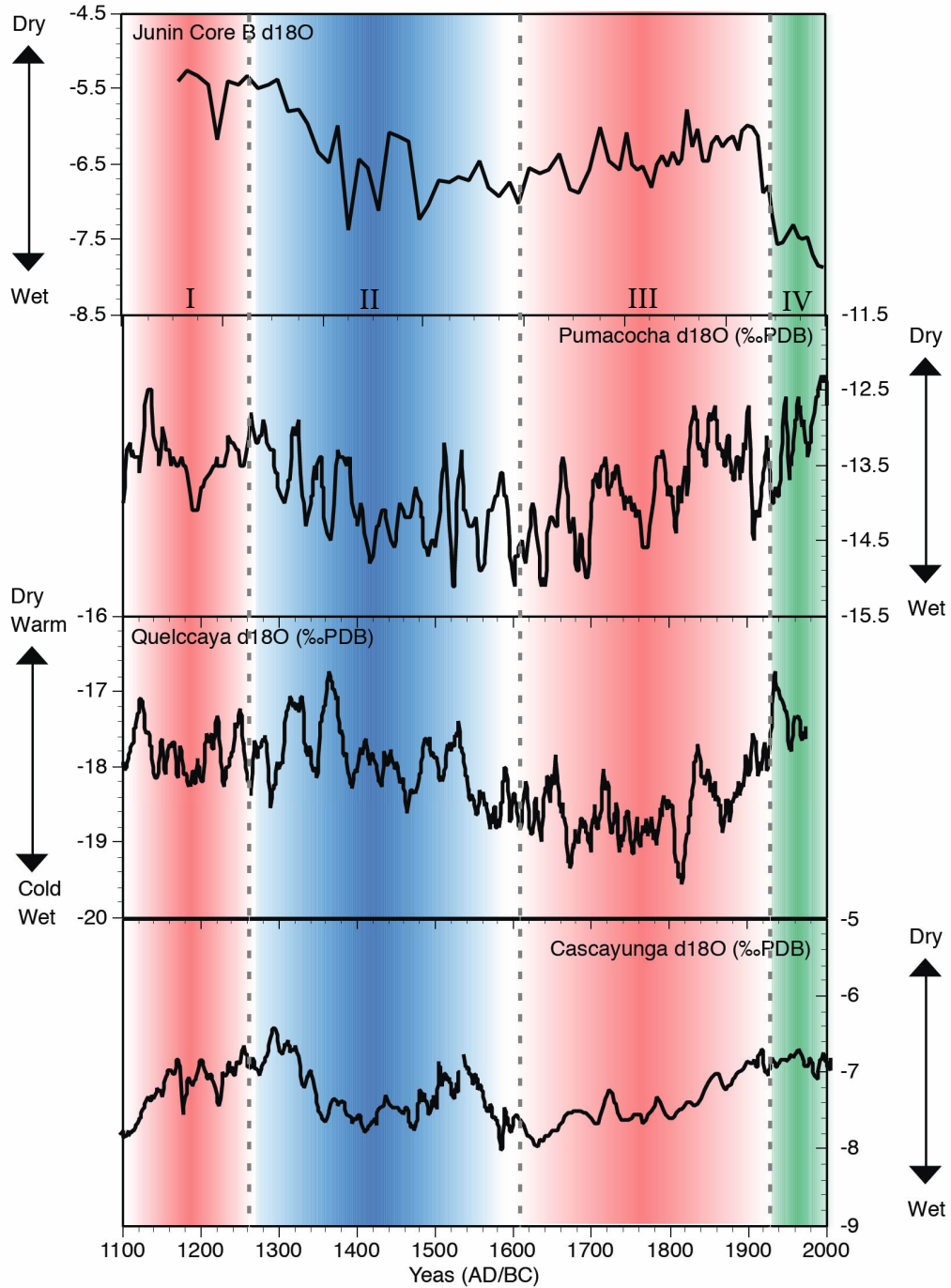


Figure 15: The Lake Junin core B  $\delta^{18}\text{O}$  record compared to the  $\delta^{18}\text{O}$  records from Pumacocha sediment core, (Bird et al. 2011a) Cascayunga speleothem record (Reuter et al. 2009) and Quelccaya ice cap (Thompson et al. 2006). The four unit divisions are labeled. The data for Pumacocha, Cascayunga and Quelccaya has been smoothed using a 5-point moving average.

### 4.3.2 Regional comparison of archive $\delta^{18}\text{O}$ records

Other archives from tropical South America exhibit similar variability in  $\delta^{18}\text{O}$  values, suggesting a regional influence of the SASM. The timing and magnitude of these events are also very similar to the Junin  $\delta^{18}\text{O}$  record. The Lake Pumacocha (10.70°S, 76.06°W, 4,300m asl) isotopic record, which is interpreted as the variability of the SASM, exhibits similar trends in  $\delta^{18}\text{O}$  values as the Junin record. The timing and magnitude of mean state changes are nearly identical through the LIA and CWP between the two records, until the Junin record deviates at 12 cm due to anthropogenic influence (Bird et al. 2011a) (Figure 15).

The Junin  $\delta^{18}\text{O}$  record also closely tracks the 900-year Cascayunga Cave  $\delta^{18}\text{O}$  record (6.09°S, 77.23°W, 930m asl). The Cascayunga speleothem record is interpreted to track annual changes in rainfall (Reuter et al. 2009). Although Cascayunga is located to the north of Junin, as well as ~3,000 m lower, the  $\delta^{18}\text{O}$  records are similar. The high resolution of the speleothem record provides better temporal constraint, while the magnitude of  $\delta^{18}\text{O}$  changes are more pronounced in the Junin record. Their similarities support the interpretation that over the past 1,000 years, the Lake Junin  $\delta^{18}\text{O}$  record has documented SASM variability (Figure 15).

The Quelccaya ice core (103.93°S, 70.83°W, 5,670m asl) and Junin core B share similar isotopic trends through the LIA and the CWP. Although the timing of the LIA occurs slightly later in the Quelccaya core, the magnitude of this event is similar between the two records. In both cores, the CWP is consistent with increasing  $\delta^{18}\text{O}$  values. The trends deviate at 1932, when the Junin core begins to record anthropogenic influence. The interpretation of the Quelccaya ice core has previously been interpreted as a paleo-temperature record, but it is now thought to

record precipitation trends on shorter time scales (Thompson et al. 1986; 2006). The similarities of the Junin, Pumacocha, Cascayunga and Quelccaya records are consistent with the interpretation that these archives record changes in tropical precipitation associated with the SASM (Figure 15).

The regional archives discussed all exhibit similar trends in  $\delta^{18}\text{O}$  values and are all in close agreement in the timing, direction and magnitude of SASM variability. From these data it is believed that SASM variability is the forcing mechanism driving the shifts in  $\delta^{18}\text{O}$  values across the Andean tropical latitudes. Although the archive sites are geographically distinct (i.e. lowland caves, high latitude ice cores), they all receive the majority of their precipitation during monsoon season, therefore explaining the synchronicity of the  $\delta^{18}\text{O}$  variability.

### **4.3.3 Sea surface temperature reconstructions and $\delta^{18}\text{O}$ records**

Northern Hemisphere (NH) SST reconstructions (Moberg et al. 2005) coupled with the Pumacocha  $\delta^{18}\text{O}$  data (Bird et al. 2011, Vuille et al. 2012) suggest a close relationship between SSTs and monsoon intensity during MCA, LIA and CWP. Oxygen isotope records from the central Andes suggest a maximum SASM intensity during the LIA, while reconstructed NH SSTs reached a 2,000-year low (Moberg et al. 2005). In contrast, a weakened mean state of the monsoon occurred during the MCA and CWP, consistent with above average reconstructed (and historical) NH temperatures (Bird et al. 2011, Moberg et al. 2005, Vuille et al. 2012). The similarities of South American tropical latitude regional archive  $\delta^{18}\text{O}$  trends validate the relationship between NH SSTs and SASM intensity.

The location of the ITCZ is believed to have an influence on the intensity of the SASM due to its sensitivity to NH temperature (Vuille et al. 2012). The ITCZ follows areas of warmest SSTs, and therefore a NH cooling would result in a southward displacement of the ITCZ. This displacement occurs due to a thermodynamic adjustment in Hadley cell circulation to allow for northward heat transport to balance the NH cooling. The location of the ITCZ is extremely important because it determines the areas that receive an enhanced moisture flux and subsequent increase in convective activity over the continental region. For example, a southward displacement of the ITCZ would result in greater convective activity over the tropical continent, as well as an enhanced moisture flux over the South American monsoon domain, resulting in greater monsoon intensity (Marengo et al. 2012). In contrast a northward displacement would cause suppressed convection over the Amazon Basin, resulting in drought-like conditions. This relationship between the ITCZ and SASM is consistent with the boreal SST cooling and intensification of the SASM (Vuille et al. 2012).

#### **4.3.4 Carbon isotope variability in Junin Core B**

In Core B, there is a large  $^{13}\text{C}$  enrichment ( $>14\text{‰}$ ) in carbonates, consistent throughout the record until  $\sim 12$  cm (1932 AD) when values drop to  $\sim 3\text{‰}$  (Figure 15). Atmospheric  $\text{CO}_2$  exchange and carbon source inputs are thought to be the main controls of authigenic carbonate values in lake sediments. However, there is a large  $^{13}\text{C}$  enrichment in carbonate lakes located on the Andean Altiplano (Valero-Garcés et al. 1999), an area that is characterized as an active geothermal area. Valero-Garcés et al. (1999) suggest that high elevation, lacustrine catchments with geothermal activity may be influenced by  $\text{CO}_2$  degassing of thermal springs, thus causing a non-equilibrium isotope fractionation. Seltzer (2000) supports this degassing interpretation,

coupled with periods of high primary productivity and sequestration of inorganic carbon in *Chara* stems. In Lake Junin, calcite typically forms around the stems of this submerged macrophyte, recording high  $\delta^{13}\text{C}$  values. *Chara* comprises most of the fine-grained calcite in the sediment record (Seltzer 2000). Other closed basin lakes in the Andean Altiplano have similar high  $^{13}\text{C}$  values (Valero-Garcés et al. 1999), suggesting a common cause for isotopic enrichment. The high  $^{13}\text{C}$  values ( $>14\text{‰}$ ) are almost exclusive to this region, and are among the highest values reported for calcite in surface waters in relevant literature. At 12 cm the  $^{13}\text{C}$  values decrease drastically to  $\sim 3\text{‰}$ . This drop is consistent with the damming of the lake and subsequent lake level rise. The Upamayo dam redirects the Rio San Juan into the lake, causing an influx of low  $\delta^{13}\text{C}$  ( $-12$  to  $-6\text{‰}$  PDB) waters to the lake (Flusche et al 2005). Therefore, a flux of isotopically low  $\delta^{13}\text{C}$  water would cause the isotopic composition of the water to shift to more negative values, as is seen in Core B.

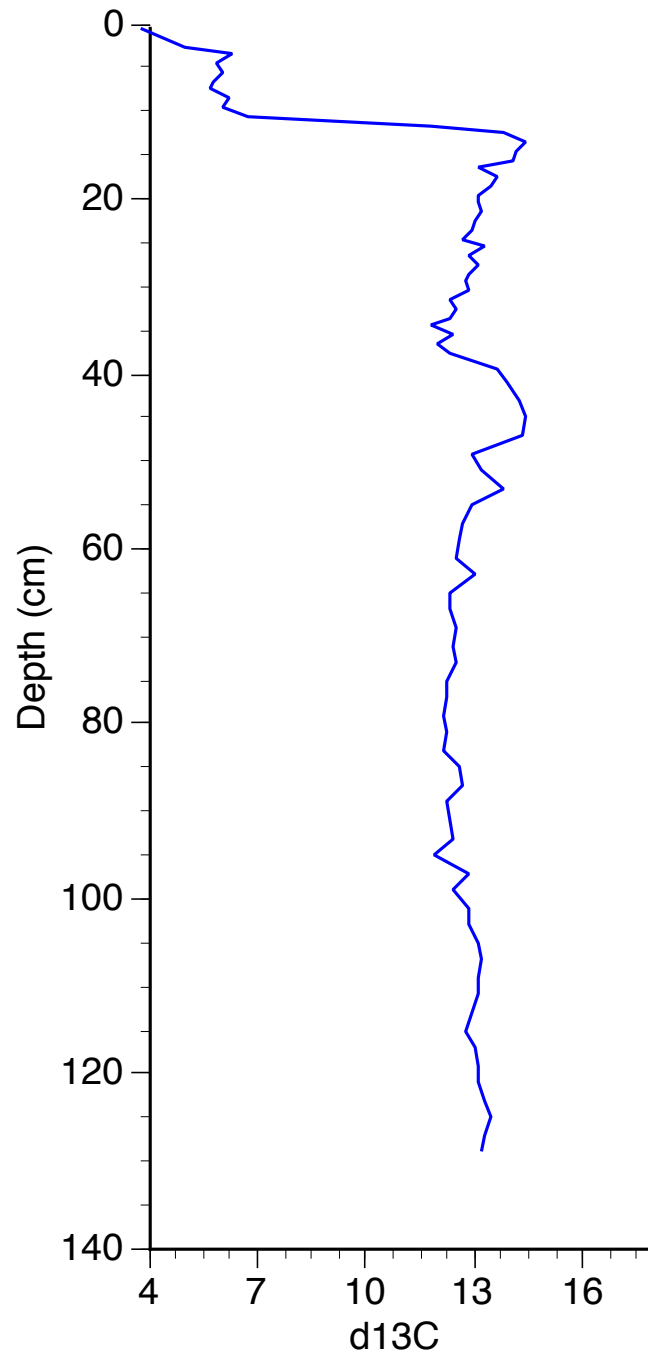


Figure 16: Junin core B  $^{13}\text{C}$  downcore variations. The  $^{13}\text{C}$  values remain very positive between 12-128 cm. The excursion to lower  $^{13}\text{C}$  values at 12cm is attributed to the construction of the Upamayo dam.  $\delta^{13}\text{C}$  measured in ppm.

## 5.0 CONCLUSIONS AND FUTURE IMPLICATIONS

Analyzing authigenic calcite precipitated in equilibrium with lake water has proved useful in reconstructing the natural variability of precipitation in the central Andes that is dominated by the South American Summer Monsoon (SASM). The Junin sediment record shows similar trends to other regional archives including ice, cave deposits and other lakes (Bird et al. 2011; Thompson et al. 1986; Thompson et al. 2006; Reuter et al. 2009; Vuille et al. 2012), supporting the hypothesis that precipitation changes occur synchronously across the region. In Junin, lower  $\delta^{18}\text{O}$  values are observed during the LIA (1250-1600 AD), supporting a strengthened SASM. Following the LIA, the CWP (1850-present) is characterized by an increase in  $\delta^{18}\text{O}$  values, suggesting a long term weakening of the SASM and associated rainfall. The SASM is influenced by the variability of the location of the ITCZ, which is controlled by the regions of warmest SSTs. This relationship suggests that a continued warming of SST during the CWP would further displace the ITCZ northward, causing an even greater reduction in SASM intensity. This reduction would negatively impact Andean glaciers and water resources, a detrimental change for many South American Cultures. The age-depth model for Lake Junin must be validated and work is in progress to do this. The timing of change is important when understanding past climatic events, and a coherent age model, supported by accurate AMS dates would improve the accuracy of this study.

Lake Junin potentially predates the maximum extent of glaciation, and contains a continuous record of tropical climate over the past hundreds of thousands of years (Rodbell 2011). Because of this unique study site and preserved sediment record, Lake Junin is currently the target of a potential deep drilling project. The aim of this project is to develop the first continuous and high resolution Quaternary record of climate change in the tropical Andes. This record would expand existing Lake Junin data have and complement other regional archives (Rodbell et al. 2011).

## BIBLIOGRAPHY

- Abbott, M. B. and Stafford, T. W., 1996: Radiocarbon Geochemistry of Ancient and Modern Arctic Lakes, Baffin Island: *Quaternary Research*, 45, 300-311.
- Abbott, M. B., Seltzer, G. O., Keltz, K. R., Southon, J., 1997: Holocene paleohydrology of the Tropical Andes from lake records: *Quat Res.*, 47, 70-80.
- Applyby, P. G., and Oldfield, F., 1983: The assessment of  $^{210}\text{Pb}$  data from sites with varying sediment accumulation rates: *Hydrobiologia*, 103, 29-35.
- Baker, P. A., Seltzer, G. O., Fritz, S. C., Dunbar, R. B., Grove, M. J., Tapia, P. M., Cross, S. L., Rowe, H.D., and Broda, J. P., 2001: The history of South American tropical precipitation for the past 25,000 years: *Science*, 291, 640-643.
- Benavides-Caceres, V., 1999: Orogenic evolution of the Peruvian Andes- The Andean cycle, Geology and ore deposits of the central Andes: Society of Economic Geologists special publication, 7, 61-107.
- Bird, B. W., Abbott, M. B., Vuille, M., Rodbell, D. T., Rosenmeier, M. F., and Stansell, N. D., 2011a: A 2300-year-long annually resolved record of the South American summer monsoon from the Peruvian Andes, *Proc. Nat. Acad. Science*
- Bird, B. W., Abbott, M. B., Rodbell, D. T., and Vuille, M., 2011b: Holocene tropical South American hydroclimate revealed from a decadal resolved lake sediment  $\delta^{18}\text{O}$  record, *Earth Planet. Sci. Lett.*, 310, 192-202.
- Blaauw, M., 2010: Methods and code for 'classical' age-modeling of radiocarbon sequences: *Quaternary Geochronology*, 5, 512-518.
- Chiang, J. C. H., and Bitz, C. M., 2005: Influence of high latitude ice cover on the marine Intertropical Convergence Zone: *Climate Dynamics*, 25, 477-496
- Cruz Jr. F. W., Karmann, I., Viana Jr., O., Burns, S. J., Ferrari, J. A., Vuille, M., Moreira, M. Z., and Sial, A. N., 2005: Stable isotope study of cave percolation waters in subtropical Brazil: implications for paleoclimate inferences from speleothems: *Chem. Geology*, 220, 245-262.

- Dansgaard, W. 1964: Stable isotopes in precipitation: *Tellus*, 16, 436–468.
- Delman, E., 2011: The history of mining in Cerro de Pasco and heavy metal deposition in Lake Junin, Peru: Union College Honors Thesis.
- Fisher, J. R., 1977: Silver mines and silver miners in colonial Peru, 1776-1824: Liverpool Centre for Latin American studies, University of Liverpool, 150.
- Flusche, M. A., Sletzer, G. O., Rodbell, D., Siegel, D., Samson, S., 2005: Constraining water sources and hydrologic processes from the isotopic analysis of water and dissolved strontium, Lake Junin, Peru: *J. of Hydrology* 312, 1-13.
- Garcia, S., and Kayano, M., 2010: Some evidence on the relationship between the South American monsoon and the Atlantic ITCZ: *Theor. Appl. Climatol.*, 99, 29–38.
- Garreaud, R., Vuille, M., and Clement, A., 2003: The climate of the Altiplano: Observed current conditions and mechanisms of past changes: *Palaeogeogr., Palaeoclimatol., Palaeoecol.*, 194, 5-22.
- Garreaud, R. D., Vuille, M., Compagnucci, R., and Marengo, J., 2009: Present-day South American climate: *Palaeogeogr., Palaeoclimatol., Palaeoecol.*, 281, 180-195.
- Kelts, K. and Hsu, K., 1978: Freshwater carbonate sedimentation: Lakes: physics, chemistry and geology, Springer, New York, 295-323.
- Lenters, J. D., Cook, K. H., 1997: On the origin of the Bolivian High and related circulation features of the South American climate: *J. Atmos. Sci.*, 54, 656-677.
- Marengo, J. A., Liebmann, B., Grimm, A. M., Misra, V., Silva Dias, P. L., Cavalcanti, I. F. A., Carvalho, L. M. V., Berbery, E. H., Ambrizzi, T., Vera, C. S., Saulo, A. C., Nogues-Paegle, J., Zipser, E., Seth, A., and Alves, L.M., 2012: Recent developments on the South American monsoon system: *International Journal of Climatology*, 32(1), 1-21.
- Moberg, A., Sonechkin, D. M., Holmgren, K., Datsenko, N. M., and Karlen, W., 2005: Highly variable northern hemisphere temperatures reconstructed from low- and high-resolution proxy data: *Nature*, 433, 613–617.
- Myrbo, A., 2004: Total inorganic carbon (TIC, carbonate) coulometry: Limnological Research Center core facility SOP series.
- O'Donnel, C., 1997: Grebes: Status survey and conservation action plan: IUNC/SSC, Grebe Specialist Group, 59.
- Rodbell, D., Abbott, M., Besonen, M., Bush, M., Colman, S., Francus, P., McGee, C., Moy, C., Polissar, P., Schwalb, A., Steinman, B., Stoner, J., Tapia, P., Valero-Garces, B., 2011: The Lake Junin (Peru) Drilling Project, ICDP proposal.

- Sachs, J. P., Sachse, D., Smittenberg, R. H., Zhang, Z., Battisti, D. S., and Golubic, S., 2009: Southward movement of the Pacific intertropical convergence zone AD 1400-1850: *Nature Geoscience*, 2, 519-525.
- Seltzer, G., Rodbell, D., and Burns, S., 2000: Isotopic evidence for late quaternary climatic change in tropical South America: *Geology*, 28(1), 35-38.
- Shanahan, T. M., Overpeck, J. T., Anchukaitis, K. J., Beck, J. W., Cole, J. E., Dettman, D. L., Peck, J. A., Scholz, C. A., and King, J. W., 2009: Atlantic forcing of persistent drought in West Africa: *Science*, 324, 377-380.
- Thompson, L. G., Davis, M. E., Mosley-Thompson, E., Sowers, T. A., Henderson, K. A., Zagorodnov, V. S., Lin, P.-N., Mikhalenko, V. N., Campen, R. K., Bolzan, J. F., Cole-Dai, J., and Francou, B., 1999: A 25,000-year tropical climate history from Bolivian ice cores: *Science*, 282, 1858-1864.
- Thompson, L. G., Mosley-Thompson, E., Brecher, H., Davis, M., Leon, B., Les, D., Lin, P.-N., Mashiotto, T., and Mountain, K., 2006: Abrupt tropical climate change: Past and present: *Proc. Nat. Acad. Science*.
- Valero-Garces, B. L., Delgado-Huertas, A., Ratto, N., Navas, A., 1999: Large  $^{13}\text{C}$  enrichment in primary carbonates from Andean Atliplano lakes, northwest Argentina: *Earth and Planetary Science Letters* 171, 253-266.
- Vimeux, F., Ginot, P., Schwikowski, M., Vuille, M., Hoffmann, G., Thompson, L. G., Schotterer, U., 2009: Climate variability during the last 1000 years inferred from Andean ice cores: a review of recent results: *Palaeogeogr. Palaeoclimatol. Palaeoecol.*, 281, 229-241.
- Vuille, M., Werner, M., Bradley, R. S., and Keimig, F. 2005: Stable isotopes in precipitation in the Asian monsoon region: *J. Geophys. Res.*, 110.
- Vuille, M., Burns, S. J., Taylor, B. L., Cruz, F. W., Bird, B. W., Abbott, M. B., Kanner, L. C., Cheng, H., and Novello, V.F., 2012: A review of the South American Summer Monsoon history as recorded in stable isotopic proxies over the past two millennia: *Clim. Past Discuss.*, 8, 637-668.
- Zhang, P., Cheng, H., Edwards, R. L., Chen, F., Wang, Y., Yang, X., Liu, J., Tan, M., Wang, X., Liu, J., An, C., Dai, Z., Zhou, J., Zhang, D., Jia, J., Jin, L., and Johnson, K., 2008: A test of climate, sun and culture relationships from an 1810-yr Chinese cave record: *Science*, 322, 940-942.
- Zhou, J., and Lau, K. M., 1998: Does a monsoon climate exist over South America?: *J. Climate*, 11, 1020-1040.